

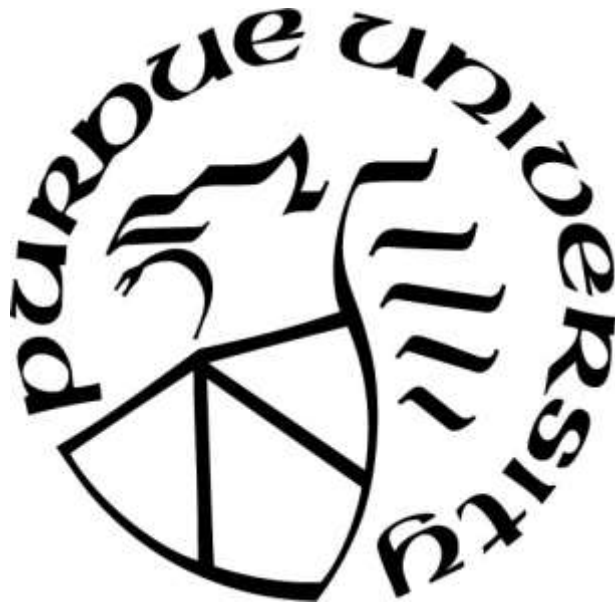
**DIFFERENTIATION AND EVALUATION OF DISEASE PROGRESSION  
IN ESSENTIAL TREMOR UTILIZING MRI BIOMARKERS**

by  
**Eric Cameron**

**A Dissertation**

*Submitted to the Faculty of Purdue University  
In Partial Fulfillment of the Requirements for the degree of*

**Doctor of Philosophy**



School of Health Sciences  
West Lafayette, Indiana  
May 2019

**THE PURDUE UNIVERSITY GRADUATE SCHOOL  
STATEMENT OF COMMITTEE APPROVAL**

Dr. Ulrike Dydak, Chair

School of Health Sciences, Purdue University

Dr. Jonathan Dyke

Department of Radiology, Weill Cornell Medicine

Dr. Carlos Perez-Torres

School of Health Sciences, Purdue University

Dr. Keith Stantz

School of Health Sciences, Purdue University

**Approved by:**

Dr. Shuang Liu

Head of the Graduate Program

*To my beloved Katie*

## ACKNOWLEDGMENTS

I would like to thank Dr. Ulrike Dydak for bringing me into her lab and for all of the wonderful help and advice along my PhD journey. Her guidance has truly helped me grow as a scholar, as well as a person. Additionally, I would like to thank all the members of Dr. Dydak's lab for their support and encouragement throughout the years.

Special thanks to Dr. Chien-Lin Yeh for teaching me so many different software tools and for always making time for my questions. Also special thanks to Dr. Elan Louis, without whose grant, I would not have had such a great project.

I am so grateful to have such a supportive and encouraging committee: Dr. Jonathan Dyke, Dr. Carlos Perez-Torres, and Dr. Keith Stantz. Thank you all for your guidance.

Thank you to everyone in the Medical Physics program at Purdue University for making my experience such a wonderful adventure.

The most thanks to my parents and my wonderful wife for always supporting my dreams.

## TABLE OF CONTENTS

LIST OF TABLES .....	7
LIST OF FIGURES .....	8
LIST OF ABBREVIATIONS .....	9
ABSTRACT .....	11
1. INTRODUCTION .....	13
1.1 Essential Tremor .....	13
1.2 Gray Matter Volume Loss .....	15
1.3 T2* Relaxometry and Iron Quantification .....	17
1.4 Specific Aims .....	18
2. GRAY MATTER DENSITY LOSS IN ESSENTIAL TREMOR: A LOBULE BY LOBULE ANALYSIS OF THE CEREBELLUM .....	20
2.1 Introduction .....	20
2.2 Methods .....	22
2.2.1 Subjects and Clinical Evaluation .....	22
2.2.2 MRI Acquisition .....	23
2.2.3 Data Processing and Analysis .....	24
2.2.4 Statistical Analysis .....	26
2.3 Results .....	27
2.4 Discussion .....	30
2.5 Conclusion .....	33
3. CEREBRAL GRAY MATTER VOLUME LOSSES IN ESSENTIAL TREMOR: A CASE- CONTROL STUDY USING HIGH RESOLUTION TISSUE PROBABILITY MAPS .....	34
3.1 Introduction .....	34
3.2 Methods .....	39
3.2.1 Clinical Assessment .....	39
3.2.2 Data Processing .....	42
3.2.3 Statistical Analysis .....	43
3.3 Method Validation .....	44
3.3.1 Smoothing Kernel .....	44

3.3.2	Method Comparison .....	48
3.4	Results.....	50
3.5	Discussion.....	52
3.6	Conclusions.....	56
4.	T2* MRI PRESENTS DIFFERENCES IN IRON DEPOSITION IN ESSENTIAL TREMOR AND PARKINSON’S DISEASE.....	57
4.1	Introduction.....	57
4.2	Methods.....	60
4.2.1	ET Study .....	60
4.2.2	PD Study 1 .....	61
4.2.3	PD Study 2.....	62
4.3	Results.....	64
4.4	Discussion.....	68
4.5	Conclusion .....	71
5.	CONCLUSIONS AND FUTURE WORK.....	72
5.1	Neurodegeneration.....	72
5.2	Disease Differentiation .....	73
5.3	Future Works .....	74
	APPENDIX.....	75
	REFERENCES .....	88

## LIST OF TABLES

- Table 2.1 Demographic data on the normal control and ET cases. The total tremor score (TTS) has a range of 0 to 36. The head/jaw tremor score (HJT) ranges from 0 to 2. The voice tremor score (VT) is binary (0 or 1). *MoCA* Montreal Cognitive Assessment, *NA* not applicable..... 28
- Table 2.2 Comparison of Lobular % GM density. Regions of significance are shown ( $p < 0.05$ ) that met the BH FDR criterion. Abberviations [*HJT* Head/Jaw Tremor (i.e., presence of head or jaw tremor on examination), *VT* Voice Tremor (i.e., presence of voice tremor on examination)]. In these comparisons, age, gender, MOCA score and group were incorporated as continuous and discrete independent variables and regressed against the regional %GM density of the 34 cerebellar regions..... 28
- Table 3.1 Chronological summary of VBM studies in essential tremor. A check mark indicates the attribute was included in the study. Abbreviations: Gray Matter (GM), ET with intention tremor (ET-I), ET with postural tremor (ET-P), control for ET-I (C-I), control for ET-P (C-P)..... 37
- Table 3.2 Demographic and clinical characteristics. P-values are with respect to controls for each group. 9M/4F ET cases were included both in the ETH and ET-ST subgroups.. 41
- Table 3.3 Summary of statistically significant regions of GM volume loss in each test. Presented p-values are on the cluster level and are deemed statistically significant using a peak-voxel p-value  $< 0.001$  and a cluster corrected threshold at the cluster level of  $p < 0.05$ . The regional specificity of the cluster is defined by one or more “peak” voxels in the cluster. Therefore, it is possible for a single cluster to belong to multiple brain regions in close proximity. Peak voxels are presented in SPM with a set of MNI coordinates that can be checked on the Automated Anatomical Labeling (AAL) atlas. ANOVA compared three groups: ET with head tremor, ET without head tremor and controls. .... 51
- Table 4.1 Demographics presented by study and respective group. Mean and standard deviation of the region of interest analysis in each group is presented by study, with linear regression p-values listed below each region by group. Note: Age and sex were used as nuisance variables in the linear regression. .... 66

## LIST OF FIGURES

Figure 2.1 A 3D representation of the segmented brainstem and cerebellum produced by SUIT ... .....	25
Figure 2.2 Overlay of the resliced subject specific SUIT template onto the GM segmented whole brain image. A) Coronal plane, B) Sagittal plane.....	26
Figure 2.3 A plot showing the % GM density within 34 cerebellar regions highlighting regions of significant decrease in ET with HJT (n = 27) and VT (n = 22) versus controls with an <i>asterisk</i> .....	29
Figure 2.4 A cerebellar atlas from SUIT is shown labelled with representative regions that showed a significant loss in %GM between control subjects and subgroups of ET subjects.....	30
Figure 3.1 ‘Glass brain’ view from SPM comparing significant clusters using three different smoothing kernels: 8 mm, 4, mm, and 2 mm. Clusters of the 4 mm smoothing kernel are closest in size to the biological change we expect. ....	47
Figure 3.2 ‘Glass brain’ view of adjusted and default method results. Gray spots are clusters of significant voxels deemed significant on a cluster-wise level. Note the lack of clusters in the cerebellum and brainstem in the adjusted results compared to the default. DARTEL results showed no significant clusters after multiple comparison correction and are not displayed. ....	49
Figure 3.3 Axial slice view of statistically significant clusters (in red). Statistical significance is determined using a peak-voxel p-value < 0.001 and a cluster corrected threshold at the cluster level of $p < 0.05$ . ANOVA was run with three groups: ET with head tremor, ET without head tremor and controls.....	52
Figure 4.1 Axial views of the T2* maps showing the globus pallidus. Due to slight differences in the imaging protocol, statistical comparisons were not performed across studies. A) ET study. B) PD study 1. C) PD study 2. ....	63
Figure 4.2 Axial views of the T2* maps showing examples of the region of interest (ROI) placements in the A) substantia nigra (SN) and B) globus pallidus (GP). This example placement is performed on a control subject from the essential tremor study.....	64
Figure 4.3 T2* values for each region plotted by group for each study for A) Left SN, B) Right SN, C) Left GP, D) Right GP. Although plotted on the same scale, no direct comparison was performed between studies. Significant group differences were found in the Right SN in PD1 and PD2. . ....	67

## LIST OF ABBREVIATIONS

AAL	Automated Anatomical Labeling
ANOVA	Analysis of Variance
BW	Bandwidth
C	Control
CHF	Congestive Heart Failure
CSF	Cerebrospinal-Fluid
ET	Essential Tremor
ETH	Essential Tremor with Head Tremor
ET-ST	Essential Tremor with Severe Tremor
FDR	False Discovery Rate
FWHM	Full Width Half Maximum
GABA	$\gamma$ -aminobutyric acid
GM	Gray Matter
GP	Globus Pallidus
GRAPPA	Generalized Autocalibrating Partial Parallel Acquisition
HJT	Head or Jaw Tremor
Hz	Hertz
ICBM	International Consortium for Brain Mapping
MCI	Mild Cognitive Impairment
MI	Myocardial Infarction
MNI	Montreal Neurologic Institute
MoCA	Montreal Cognitive Assessment
MPRAGE	Magnetization Prepared Rapid Acquisition Gradient Echo
MRI	Magnetic Resonance Imaging
OA	Osteoarthritis
PET	Positron Emission Tomography
PD	Parkinson's Disease
QSM	Quantitative Susceptibility Mapping
ROI	Region of Interest

SCA	Spinocerebellar Ataxia
SN	Substantia Nigra
SNR	Signal to Noise Ratio
SPECT	Single Photon Emission Computed Tomography
SUIT	Spatially Unbiased Infra-Tentorial Template
T	Tesla
T1	Spin-Lattice Relaxation Time, Longitudinal Relaxation Time
T2	Spin-Spin Relaxation Time, Transverse Relaxation Time
TE	Echo Time
TI	Inversion Time
TIA	Transient Ischemic Attack
TPMs	Tissue Probability Maps
TR	Repetition Time
TTS	Total Tremor Score
UPDRS	Unified Parkinson's Disease Rating Scale
VBM	Voxel-Based Morphometry
VOI	Volume of Interest
VT	Voice Tremor
WHIGET	Washington Heights-Inwood Genetic Study of Essential Tremor
WM	White Matter

## ABSTRACT

Author: Cameron, Eric M. PhD

Institution: Purdue University

Degree Received: May 2019

Title: Differentiation and Evaluation of Disease Progression in Essential Tremor Utilizing MRI Biomarkers.

Committee Chair: Ulrike Dydak

Essential tremor (ET) is one of the most common movement disorders, characterized by kinetic tremor in the upper extremities with additional cranial tremor often present in the neck or jaw. While it is well established that ET is primarily a cerebellar disorder, recent investigations have shown more widespread pathological effects throughout the brain. Furthermore, the neurodegenerative nature of ET is still disputed and requires additional investigation. Additionally, the link between ET and Parkinson's disease (PD) is of special interest, as it can be challenging to clinically differentiate these diseases.

While post-mortem studies have helped to further the pathological understanding of these diseases, non-invasive in-vivo techniques allow for more accurate diagnosis in the clinic. With a more accurate diagnosis comes a more targeted treatment, and hopefully an improved remediation of the disease. My thesis seeks to further investigate the neurodegenerative hypothesis of ET as well as explore magnetic resonance imaging (MRI) biomarkers for potential differences in ET and PD.

These aims will be accomplished in three steps. First, gray matter volume loss in the cerebellum was investigated using voxel-based morphometry and the Spatially Unbiased Intra-Tentorial Template (SUIT) atlas on a lobule level. High resolution 3D T1-weighted MRI images were acquired on 47 ET cases and 36 controls. The cerebellum was segmented into 34 lobules using the SUIT atlas. Percent gray matter was calculated as the ratio of lobule gray matter volume divided by total lobule volume. No significant differences were identified between ET cases and controls in any of the 34 lobules. However, nine lobules had significantly decreased percent gray matter in ET cases with head or jaw tremor ( $n = 27$ ) compared to controls. Also, 11 lobules had significantly decreased percent gray matter in ET cases with voice tremor ( $n = 22$ ) compared to controls. This result confirms, with increased regional accuracy, gray matter volume loss in the cerebellum of ET cases.

Second, gray matter volume loss beyond the cerebellum, in the cerebrum, was investigated using voxel-based morphometry. High resolution 3D T1-weighted MRI images were acquired on 47 ET cases and 36 controls for processing in SPM12. The processing steps of SPM12 were updated to include a higher resolution atlas and set of tissue probability maps to optimize the segmentation and normalization of each subject image. After segmentation, normalization, and smoothing, a voxel-wise statistical analysis was performed to identify clusters of gray matter volume in ET cases compared to controls. ET cases showed decreased gray matter volume in the bilateral superior temporal region and the anterior and posterior cingulate cortex. These results, in combination with previous work provide support of wide-spread neurodegeneration in ET using optimized methodology.

Third, we applied T2\* mapping to determine relative iron concentrations in the substantia nigra (SN) and globus pallidus (GP) in ET and PD cases. Three separate studies were independently investigated to validate the reproducibility and detectability of group differences using T2\* mapping. The first study (ET study) acquired T2\* maps on 21 ET cases and 12 matched controls, the second study (PD study 1) acquired T2\* maps on 10 PD cases and 7 controls, and the third study (PD study 2) acquired T2\* maps on 21 PD cases and 17 controls. Regions of interest (ROIs) were manually placed in the SN and GP for each subject and group differences were calculated independently for each study using a linear regression model with age and sex as covariates. A significant decrease in T2\* was found in PD study 1 and PD study 2 in the right SN in PD cases compared to their respective controls, indicating increased iron deposition. No significant difference was found in the ET group compared to their respective controls in the SN. No significant differences were found in any of the three studies in the GP. These results provide evidence for a difference in brain iron regulation in the pathology of ET and PD.

Together, these thesis aims provide additional evidence in support of the neurodegenerative hypothesis of ET using updated methodology and present a quantitative imaging difference between groups of ET and PD cases.

# 1. INTRODUCTION

## 1.1 Essential Tremor

Essential Tremor (ET) is one of the most common neurological movement disorders, occurring in an estimated 0.9% of the population (all ages) (Louis, 2010). Clinically, the disease presents with a 4 – 12 Hz kinetic tremor in the upper extremities, and often develops head and voice tremor with disease progression (Benito-León & Labiano-Fontcuberta, 2016). ET is thought to be a larger family of diseases with additional motor and non-motor symptoms, such as gait ataxia, cognitive impairment, and sleep disorders. Although the disease can present with heterogeneous pathological and clinical features, the presence of the kinetic tremor is a characteristic trait of the disease (Benito-León & Labiano-Fontcuberta, 2016). Importantly, this kinetic tremor typically presents with an intentional component, meaning that as a subject nears the target of their motion, the kinetic tremor increases in amplitude.

The cerebellum has been shown to be essential in maintaining smooth, continuous motion. Specifically, there is a complex interaction between sensory input and motor output in the cerebellum that continuously update motion based on predicted sensory consequences. The ability to regulate motion with respect to predicted sensory outcomes has also been shown to be impaired in cases with cerebellar damage (Blakemore, Chris, & Wolpert, 2001; Statton, Vazquez, Morton, Vasudevan, & Bastian, 2018). Therefore, the presence of an intention tremor, among other symptoms, in ET is suggestive of cerebellar dysfunction (Benito-León & Labiano-Fontcuberta, 2016).

The cerebellum is thought to be the primary seat of the disease in ET, having been implicated in both imaging and post mortem studies. Although other brain regions are also of interest in the neuropathology of ET, such as the red nucleus, thalamus, inferior olivary nucleus,

basal ganglia, and motor cortex (Louis et al., 2007). Specifically in the cerebellum, there has been shown to be a 5- to 6-fold increase in torpedoes (fusiform swellings of Purkinje cell axon) as well as a significant reduction of Purkinje cells in post-mortem brain slices in ET cases compared to control brains (Louis et al., 2007).

While ET is widely acknowledged to be a cerebellar disease, whether it is neurodegenerative in nature is still actively investigated. The primary focus of many studies is the Purkinje cell layer in the cerebellum, specifically investigating the loss of Purkinje cells (Choe et al., 2016; Louis et al., 2007; Rajput, Robinson, Rajput, Robinson, & Rajput, 2012; Symanski et al., 2014). Purkinje cells are a major storage site for the primary inhibitory neurotransmitter  $\gamma$ -aminobutyric acid (GABA) and therefore play a crucial role on cerebellar motor control. Additionally, some clinical motor symptoms of ET coincide with symptoms of other neurodegenerative disorders (such as Parkinson's disease and Alzheimer's disease), as well as cognitive deficits (Benito-León, 2014). The similarity between ET and other neurodegenerative diseases, as well as reported Purkinje cell loss, provides evidence for the neurodegenerative hypothesis in ET. Post-mortem and neuroimaging studies have investigated many facets of disease pathology such as neuronal (volume) loss and metabolic changes in the brain, many focusing on the cerebellum (Louis et al., 2007; Louis, Huang, Dyke, Long, & Dydak, 2014).

There is also a lot of active investigation into the link between ET and Parkinson's disease (PD). PD presents with a diverse set of both motor and non-motor symptoms, such as bradykinesia, rigidity, dystonia, and mood disorders. As ET can often present with some of these same symptoms, these two diseases can be challenging to distinguish clinically, and it is thought that cases with ET are at heightened risk of developing PD (Tarakad & Jankovic, 2018). Of

course, the gold standard for PD diagnosis is the finding of Lewy bodies in the substantia nigra upon autopsy, which is not seen in a typical ET autopsy (Louis et al., 2007). Further, there are some pathological similarities between the two diseases, such as an increase in torpedoes (swollen Purkinje cell axons). In contrast, cerebellar atrophy has been shown to occur only in ET cases, not in PD. Finally, while Lewy bodies are sometimes present in ET brains, they are typically restricted to the locus ceruleus. Lewy bodies are widespread throughout PD brains, again, accumulating most noticeably in the substantia nigra (Tarakad & Jankovic, 2018). With additional imaging biomarkers, these two diseases could be further differentiated clinically, and treatments used more effectively to target the identified disease.

## **1.2 Gray Matter Volume Loss**

Gray matter (GM) volume loss is representative of substantial cellular death in the brain, specifically neuronal death, and is a defining trait of neurodegeneration. While ET is hypothesized to be neurodegenerative, there is still active debate over whether there is physical cell death, rather than just cellular dysfunction (Louis et al., 2014). As previously mentioned, there have been post-mortem studies showing significant Purkinje cell loss in the cerebellum of ET cases, in support of the neurodegenerative hypothesis. Furthermore, multiple studies have investigated GM volume loss in ET using voxel-based morphometry (VBM), in both the cerebellum and cerebrum. However, these studies have reported mixed results due to differences in population size, condition severity, and specifics of the VBM processing method (Bagepally et al., 2012; Benito-León et al., 2009; Bhalsing et al., 2014; Buijink et al., 2015; Daniels et al., 2006; Lin et al., 2013; Nicoletti et al., 2015). Therefore, further investigation into GM volume loss in ET is warranted with improved methodology.

VBM is a computation method that allows for the study of structural changes to be assessed on a voxel-wise basis in a set of magnetic resonance imaging (MRI) data. Specifically applied to GM maps, it can identify regions of GM volume loss in a subject population. Briefly, VBM requires an input of a high-resolution T1 weighted MRI image, which is segmented into three tissue classes: GM, white matter (WM), and cerebrospinal fluid (CSF). This segmentation is accomplished using a Bayesian approach which requires a prior probability map for each tissue. These prior probability maps are warped into subject space for each individual subject to create subject-specific tissue maps. Following segmentation, the T1-weighted images must be normalized to a common atlas space. This normalization is then applied to the GM tissue map. Importantly, the normalization process includes an intensity correction, which modulates the image intensity of the GM images by an amount proportional to the volume change of each voxel. For example, if a voxel doubles in volume, the intensity is halved, to ensure that voxel represents the same amount of tissue in the transformed space. Finally, images should be smoothed to increase the normality of the data for statistical comparison (Ashburner, 2009; Ashburner & Friston, 2000, 2005). Statistics can be performed on a voxel-wise basis, and comparison for multiple correction should be performed using extent cluster thresholding (Friston et al., 1995; Friston, Worsley, Frackowiak, Mazziotta, & Evans, 1994).

While this method segments the whole brain, modified processing is needed to specifically investigate GM volume changes in the cerebellum. Normalization of the whole brain to a standard space can sometimes warp the cerebellum slightly out of alignment to maximize the fit of the cerebrum to the standard template. This issue can be mitigated however, if the cerebellum and brainstem are first isolated from the cerebrum for each subject. Then this isolated cerebellum can be normalized to a cerebellum specific atlas. This can be achieved using the

SUIT toolbox in SPM12 (University College London, Wellcome Trust Centre for Neuroimaging, UK) which utilizes the Spatially Unbiased Infra-tentorial Template of the cerebellum and brainstem (Diedrichsen, 2006). Together these methods allow for separate investigation of the extent of GM volume loss in the cerebellum and cerebrum of ET cases.

### **1.3 T2\* Relaxometry and Iron Quantification**

MRI has two relaxation time constants that relate to the signal of the spinning protons: spin-lattice relaxation time or longitudinal relaxation time (T1), and spin-spin relaxation time or transverse relaxation time (T2). The T2 relaxation time is related to the dephasing of the proton signal in the transverse plane after excitation and is associated with the interaction between protons. This dephasing is further affected by macroscopic magnetic field inhomogeneities, which is termed T2'. T2\* is a combined effect of T2 and T2' ( $1/T2^* = 1/T2 + 1/T2'$ ), with T2\* being directly measurable with MRI.

T2\* is specifically sensitive to the presence of ferromagnetic molecules in close proximity to the water protons. The presence of ferromagnetic molecules, such as iron, alters the T2\* relaxation time of the surrounding tissue. In turn, this alteration of T2\* can be measured and serves as a relative quantification of the local iron concentrations in the tissue. Specifically, T2\* decreases with an increase of local iron, so the lower the T2\* signal, the greater the iron concentration.

The role of iron in neurodegeneration in PD has been widely studied, and has been well documented to show increased iron accumulation in the substantia nigra, among other regions (Dexter et al., 1987; Zecca, Youdim, Riederer, Connor, & Crichton, 2004). More recent studies have reported the utility of quantitative imaging methods such as T2\* relaxometry and quantitative susceptibility mapping (QSM) in detecting iron deposition throughout the brain in

PD (Langkammer et al., 2016; Ulla et al., 2013). In ET however, only one study so far has investigated iron deposition (Novellino et al., 2013). With iron deposition being an indicator for many neurodegenerative disorders, and specifically for PD, further investigation into iron and ET is warranted (Ward, Zucca, Duyn, Crichton, & Zecca, 2014).

#### **1.4 Specific Aims**

Although ET is one of the most common movement disorders, the causes and pathological markers of the disease are not fully understood. Although post-mortem studies provide end-stage disease pathology, advance imaging methods can be applied to help gain a better understanding of disease state and progression in-vivo.

Therefore, my central hypothesis is that MRI can be used to assess the neurodegenerative extent of ET as well as investigate pathophysiological differences between ET and PD. My dissertation aims to address this hypothesis by investigating gray matter volume loss in the cerebellum and cerebrum and to investigate the differences in regional brain iron deposition between ET and PD using T2\* mapping. To test our hypothesis, we propose the following Specific Aims:

##### **Aim 1:**

*To test the hypothesis of neurodegeneration in the cerebellum in Essential Tremor seen by gray matter density loss using a lobule by lobule methodology.*

This aim will be achieved using MRI and the SUI toolbox with voxel-based morphometry in a cohort of ET cases and controls (chapter 2).

##### **Aim 2:**

*To test the hypothesis that neurodegeneration in Essential Tremor extends beyond the cerebellum seen by gray matter volume loss in the cerebrum.*

This aim will be achieved using MRI and voxel-based morphometry in a cohort of ET cases and controls (chapter 3).

**Aim 3:**

*To test the hypothesis of increased brain iron accumulation, comparing Essential Tremor and Parkinson's disease through T2\* relaxometry as a potential disease differentiating biomarker.*

This aim will be accomplished using MRI T2\* mapping to quantify iron levels in a subset of the ET cases and controls, which will be further compared to two separate cohorts of PD cases and controls (chapter 4).

## 2. GRAY MATTER DENSITY LOSS IN ESSENTIAL TREMOR: A LOBULE BY LOBULE ANALYSIS OF THE CEREBELLUM

*Published in Cerebellum & Ataxias (2017) 4:10*

*Jonathan P. Dyke, Eric Cameron, Nora Hernandez, Ulrike Dydak, Elan D. Louis*

*Eric Cameron contributed in method development and optimization, data processing and statistical analysis.*

### 2.1 Introduction

Essential tremor (ET) is a neurological disease whose chief clinical feature is kinetic tremor of the arms; it is the most common tremor disorder in humans (Louis & Ottman, 2014; “Tremor Fact Sheet,” 2017). The pathophysiological basis for ET is still under active investigation, although evidence increasingly links it to a disordered and perhaps degenerative cerebellum (Grimaldi & Manto, 2013; Louis et al., 2014). Multi-modality neuroimaging studies have used Magnetic Resonance Imaging (MRI), Positron Emission Tomography (PET) and Single Photon Emission Computed Tomography (SPECT) to study structural and metabolic changes in ET (Klaming & Annese, 2014; Sharifi, Nederveen, Booiij, & van Rootselaar, 2014). These studies have reported metabolic and structural changes in the cerebellum (Louis et al., 2002; Quattrone et al., 2008; Shin et al., 2016). However, they have yielded conflicting results with regards to generalized cerebellar atrophy. Hence, further study is needed.

Voxel based morphometry (VBM) is frequently used to identify clusters of voxels with differing percentage gray matter (%GM) density. These clusters are determined through statistical analysis and frequently overlap specific anatomical boundaries of individual cerebellar lobules. Our study accurately identifies contributions of %GM density change within specific

cerebellar lobules of interest by using a Spatially Unbiased Infra-tentorial Template (SUIT) of the cerebellum and brainstem (Diedrichsen & Zotow, 2015). This atlas was normalized on a subject specific basis to the GM segmented data and the %GM density was quantified in each cerebellar lobule. The %GM density is assumed to be a close proxy of brain atrophy and has been used to quantitate the degree of neurodegeneration in Alzheimer's and Parkinson's disease (Chen et al., 2016; Frisoni et al., 2002). We postulate that our lobule by lobule approach may better distinguish changes in %GM density in subjects with ET from controls or subtypes of ET from controls.

Our study also included a detailed clinical evaluation of ET patients, which allowed us to assess multiple phenotypic features. These included the severity of action tremor (total tremor score, TTS), the presence of head (i.e., neck) or jaw tremor, and the presence of voice tremor. As cognitive dysfunction has been associated with ET as well, we administered the Montreal Cognitive Assessment (MoCA) score, a measure of global cognitive function. Detailed phenotyping is important as there is a sense that ET may be a family of diseases rather than a unitary entity, and etiological and pathophysiological features could track with certain phenotypes (Louis, 2014).

Aside from possible diagnostic value, the current technique has the potential to be applied to serial studies to assess disease progression as a function of time. Knowledge of specific cerebellar lobule degeneration may also be used to localize pathways and models of disease within the cerebellum as linked to tremor.

## 2.2 Methods

### 2.2.1 Subjects and Clinical Evaluation

Forty-seven ET cases (24 M/23F, age  $76.0 \pm 6.8$  years, TTS  $20.3 \pm 6.2$ , MoCA score  $27.5 \pm 2.2$ ) and 36 normal control subjects (10 M/26F, age  $73.2 \pm 6.7$  years, TTS  $5.3 \pm 2.5$ , MoCA score  $28.1 \pm 1.7$ ) were recruited for this study. The average age of onset of ET was  $40.3 \pm 21.5$  years with a range from 5 to 75 years, and 5 ET subjects having an age of onset  $\geq 65$  years. This sample size was well within the range of that of prior volumetric studies of ET (e.g., 10 ET cases and 13 controls (Lin et al., 2013), 19 ET and 19 controls (Gallea et al., 2015), 39 ET cases and 36 controls (Shin et al., 2016)). The study protocol was reviewed and approved by the Yale, Cornell and Purdue Human Subjects Institutional Review Boards. Written informed consent was obtained from each subject prior to participation in the study.

ET cases were recruited from a clinical-epidemiological case-control study of ET, one of the author's (E.D.L.) neurological practices and study advertisements (Louis, Hernandez, Dyke, Ma, & Dydak, 2016). Inclusion criteria were a diagnosis of ET from a treating neurologist and a willingness to undergo an MRI scan. Exclusion criteria included heavy exposure to ethanol (as defined previously) (Harasymiw & Bean, 2001), a history of a neurodegenerative disease (Alzheimer's disease, Parkinson's disease, etc.), prior deep brain stimulation or other neurosurgery or a contraindication for MRI. Normal control subjects were recruited during the same time period and from the same sources as the ET cases with some being spouses of the ET cases. They were matched to ET cases based on age. As cases were more readily available, their recruitment occurred more easily than those of controls, and this contributed to an unequal number of cases and controls. Exclusion criteria for controls included a history of ET and a family history of ET (i.e., a reportedly affected first-degree or second-degree relative).

An in-person assessment was performed by a trained research assistant. Demographic and clinical data were collected and, as cognitive deficits have been reported in ET, the Montreal Cognitive Assessment (MoCA) was performed as a brief assessment of cognitive function (Nasreddine et al., 2005). During the in-person assessment, a videotaped neurological examination was also performed on all cases and controls. This included one test for postural tremor and five for kinetic tremor (12 tests total) as well as sustained phonation, conversational speech and a reading aloud task. A senior neurologist specializing in movement disorders (E.D.L.) used a reliable and valid clinical rating scale, the Washington Heights-Inwood Genetic Study of Essential Tremor (WHIGET) rating scale (Louis, Ford, Lee, Andrews, & Cameron, 1998), to rate postural and kinetic tremor during each test: 0, 0.5, 1, 1.5, 2 and 3, resulting in a total tremor score (range, 0–36). Head (i.e., neck) and jaw tremors were noted as present or absent on examination, and a head/jaw tremor score was assigned to each case [0 = Absent, 1 = Present in Head or Jaw, 2 = Present in Head and Jaw]. In addition, voice tremors were noted as present or absent on examination. Diagnoses of ET were re-confirmed by the neurologist (E.D.L.) based on the history and videotaped neurological examination. WHIGET diagnostic criteria were applied (moderate or greater amplitude kinetic tremor [tremor rating  $\geq 2$ ]) during three or more tests or the presence of a head tremor, in the absence of Parkinson's disease, dystonia or another cause.

### **2.2.2 MRI Acquisition**

MRI exams were performed on a 3.0 Tesla Siemens Tim Trio scanner (Siemens Healthcare, Erlangen, Germany), equipped with a 32-channel head coil. All scans were performed at Weill Cornell Medicine at the Citigroup Biomedical Imaging Center. In order to determine voxel tissue composition and account for partial volume components, high-resolution

MPRAGE images were acquired (TR/TE/TI = 2300/2.91/900 ms, flip angle = 9°, bandwidth: 240 Hz/pixel, voxel size: 1.0mm× 1.0mm× 1.2mm, GRAPPA = 2).

### 2.2.3 Data Processing and Analysis

MRI data processing was performed using SPM12 (University College London, Wellcome Trust Centre for Neuroimaging, UK) using the SUIT toolbox (Ashburner & Friston, 2000). This refers to the Spatially Unbiased Infra-tentorial Template of the cerebellum and brainstem (Diedrichsen, 2006). SPM12 was specifically chosen as previous versions (SPM5, SPM8) were noted to stretch the cerebellum in the z-direction during the normalization procedure. The first step was to “isolate” the cerebellum and brainstem using the SUIT toolbox on the high resolution T1-Weighted MPRAGE images (Fig. 2.1). Gray matter segmentation was performed within SPM using a modified Gaussian mixture model. This model segments GM voxels based on likelihood and prior probability maps compiled from a large sample set.

The next step was to normalize or deform each cerebellum and brainstem into the SUIT atlas template. This procedure aligns individual fissures and reduces their spatial spread as well as improves on alignment of the deep cerebellar nuclei. The atlas contains 34 lobes in the left, right and vermal regions (Diedrichsen, Balsters, Flavell, Cussans, & Ramnani, 2009). The following 13 regions were defined in the left and right cerebellum, respectively: Crus I, Crus II, Dentate, Fastigial, Interposed, I-IV, V, VI, VIIb, VIIIa, VIIIb, IX, X. The following 8 regions were defined in the vermis: Crus I, Crus II, VI, VIIb, VIIIa, VIIIb, IX, X. Once the normalization matrix was determined, the final step inverted the transformation and resliced the SUIT cerebellar atlas back into subject space. This produced a subject specific cerebellar atlas with the number of voxels in each lobule converted back to a volume in cc knowing the voxel size of 1.0 mm × 1.0 mm × 1.2 mm.

The volume of each lobule in the atlas contained contributions from GM, white matter (WM) and cerebrospinal fluid (CSF). Any changes in GM density caused by cerebellar atrophy might be masked by lesser changes in absolute lobular volume which may occur with normal aging. The GM segmented map was resliced in SPM to match the matrix size of the subject specific SUIIT atlas (Fig. 2.2). Code was written in-house (J.P.D.) using IDL 8.1 (Exelis Visual, Broomfield, CO) to mask each lobule in the SUIIT atlas and multiply by the GM segmented image. The sum of all voxel values in the resulting image product represented the total GM volume within each lobule. A final quantitative ratio of GM volume/total lobular volume yielded the exact %GM density in each lobule. This ratio was independent of the size of the lobule and could be compared across groups.

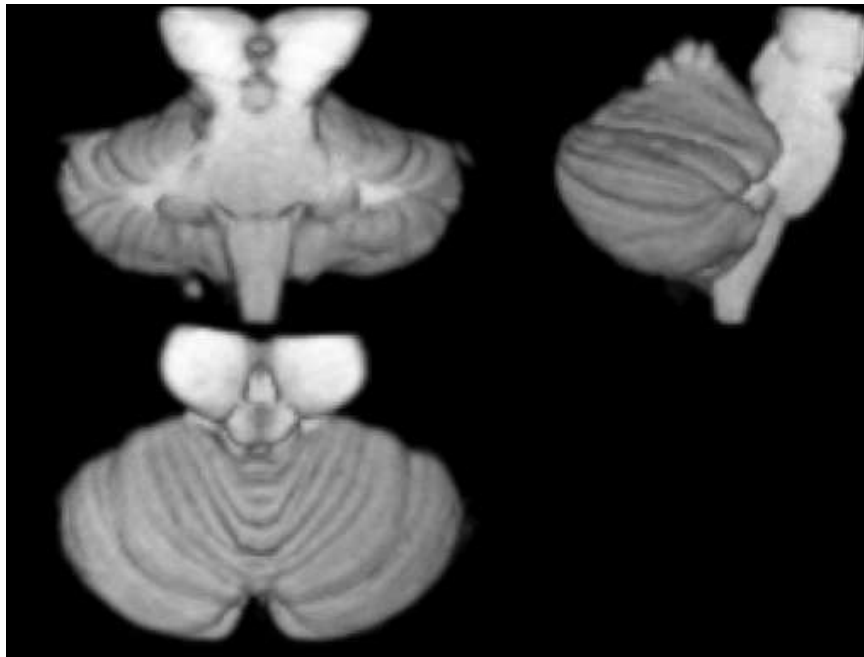


Figure 2.1 A 3D representation of the segmented brainstem and cerebellum produced by SUIIT



Figure 2.2 Overlay of the resliced subject specific SUI template onto the GM segmented whole brain image. A) Coronal plane, B) Sagittal plane.

#### 2.2.4 Statistical Analysis

All analyses were performed in R (version 3.3.2). We used Student's t tests to compare the features of ET cases vs. control subjects. Linear regression models were performed with the %GM density from each of the 34 cerebellar regions as the outcome, with group (control vs. ET), age, gender and MOCA score as independent predictors. The Benjamini-Hochberg method was used to calculate the False Discovery Rate (FDR) and correct for multiple comparisons (Benjamini & Hochberg, 1995; Glickman, Rao, & Schultz, 2014). Statistical tests resulting in  $p < 0.05$  were considered significant with an FDR cutoff of ( $\alpha = 0.1$ ). In additional models, we compared three phenotypically-defined subgroups of ET cases to controls (i.e., ET cases with head or jaw tremor (HJT), ET cases with voice tremor (VT), and ET cases with severe arm tremor defined by the upper quartile of TTS [ $\geq 23$ ]).

### 2.3 Results

ET cases and controls did not differ significantly with respect to age ( $p = 0.062$ ) or MOCA score ( $p = 0.116$ ) (Table 2.1). There was a slight difference with respect to gender ( $p = 0.03$ ) in the control group, which was accounted for in the regression model. In these comparisons, age, gender, MoCA score and group were incorporated as continuous and discrete independent variables and regressed against the regional %GM density of the 34 cerebellar regions.

Comparing the %GM density in all ET vs. control subjects resulted in no significant differences after correction for multiple comparisons. In additional models, we compared three phenotypically-defined subgroups of ET cases to controls. When compared with controls, ET cases with head or jaw tremor (HJT;  $n = 27$ ) showed significant decreases in %GM density that met the BH FDR criterion in the following regions, presented in order of significance: Right\_IX ( $p = 0.001$ ), Left\_V ( $p = 0.004$ ), Left\_VIIIa ( $p = 0.009$ ), Left\_IX ( $p = 0.010$ ), Vermis\_VIIb ( $p = 0.011$ ), Left\_VIIb ( $p = 0.013$ ), Left\_X ( $p = 0.014$ ), Left\_I\_IV ( $p = 0.018$ ) and Right\_V ( $p = 0.021$ ) (Table 2.2). Compared to controls, ET cases with voice tremor (VT;  $n = 22$ ) exhibited significant decreases in %GM density that met the BH FDR criterion in the following regions, presented in order of significance: Right\_IX ( $p = 0.001$ ), Vermis\_VIIb ( $p = 0.004$ ), Left\_IX ( $p = 0.005$ ), Left\_V ( $p = 0.006$ ), Left\_X ( $p = 0.008$ ), Vermis\_CrusII ( $p = 0.012$ ), Vermis\_CrusI ( $p = 0.016$ ), Vermis\_VI ( $p = 0.019$ ), Left\_I\_IV ( $p = 0.025$ ), Vermis\_VIIIb ( $p = 0.026$ ) and Right\_V ( $p = 0.026$ ) (Table 2.2). Lastly, ET cases with severe tremor ( $TTS \geq 23$ ;  $n = 20$ ) showed no significant decreases compared to controls after correcting for multiple comparisons. The average %GM density for each region comparing all ET ( $n = 47$ ) and control subjects ( $n = 36$ ) is plotted in Fig. 2.3; the asterisks label significant regions of decreased %GM in ET with HJT ( $n = 27$ ) and VT ( $n = 22$ ) versus controls (Table 2.2). Figure 2.4 labels representative lobules of significant decrease between control subjects and subgroups of ET subjects.

Table 2.1 Demographic data on the normal control and ET cases. The total tremor score (TTS) has a range of 0 to 36. The head/jaw tremor score (HJT) ranges from 0 to 2. The voice tremor score (VT) is binary (0 or 1). *MoCA* Montreal Cognitive Assessment, *NA* not applicable

	<b>Controls</b>	<b>(n=36)</b>	<b>ET</b>	<b>(n=47)</b>		
	<b>Mean</b>	<b>Stdev</b>	<b>Mean</b>	<b>Stdev</b>	<b>t</b>	<b>P</b>
<b>Age</b>	73.1	6.7	76.0	6.8	-1.90	0.062
<b>Gender</b>	10M/26F		24M/23F		2.20	0.030
<b>MOCA</b>	28.1	1.7	27.4	2.5	1.59	0.116
<b>Age of Onset</b>	0.0	0.0	41.0	20.7		-
<b>HJT</b>	0.0	0.0	1.0	1.1		-
<b>VT</b>	0.0	0.0	0.5	0.5		-
<b>TTS</b>	5.3	2.5	20.4	6.2	-15.21	<0.0001

Table 2.2 Comparison of Lobular % GM density. Regions of significance are shown ( $p < 0.05$ ) that met the BH FDR criterion. Abbreviations [*HJT* Head/Jaw Tremor (i.e., presence of head or jaw tremor on examination), *VT* Voice Tremor (i.e., presence of voice tremor on examination)]. In these comparisons, age, gender, MOCA score and group were incorporated as continuous and discrete independent variables and regressed against the regional %GM density of the 34 cerebellar regions.

	<b>ET w/HJT vs. Controls</b> <b>n = 27 vs n = 36</b>	<b>ET w/VT vs. Controls</b> <b>n = 22 vs n = 36</b>
<b>Left_I-IV</b>	(p = 0.018)	(p = 0.025)
<b>Left_V</b>	(p = 0.004)	(p = 0.005)
<b>Left_VIIIb</b>	(p = 0.013)	
<b>Left_VIIIa</b>	(p = 0.009)	
<b>Left_IX</b>	(p = 0.010)	(p = 0.005)
<b>Left_X</b>	(p = 0.014)	(p = 0.008)
<b>Right_V</b>	(p = 0.021)	(p = 0.026)
<b>Right_IX</b>	(p = 0.001)	(p = 0.001)
<b>Vermis_CrusI</b>		(p = 0.016)
<b>Vermis_CrusII</b>		(p = 0.012)
<b>Vermis_VI</b>		(p = 0.019)
<b>Vermis_VIIIb</b>	(p = 0.011)	(p = 0.004)
<b>Vermis_VIIIb</b>		(p = 0.026)

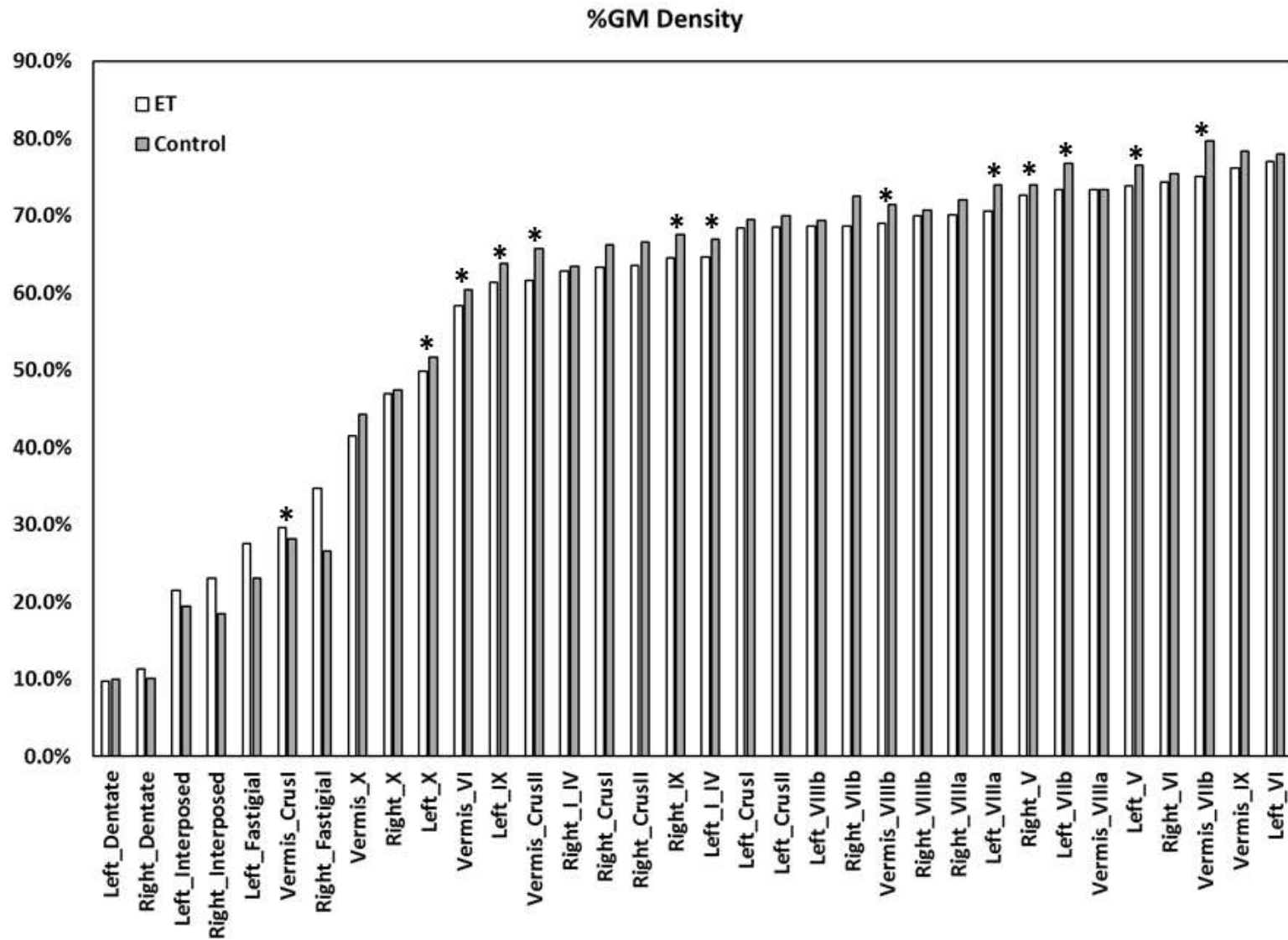


Figure 2.3 A plot showing the % GM density within 34 cerebellar regions highlighting regions of significant decrease in ET with HJT (n = 27) and VT (n = 22) versus controls with an *asterisk*.

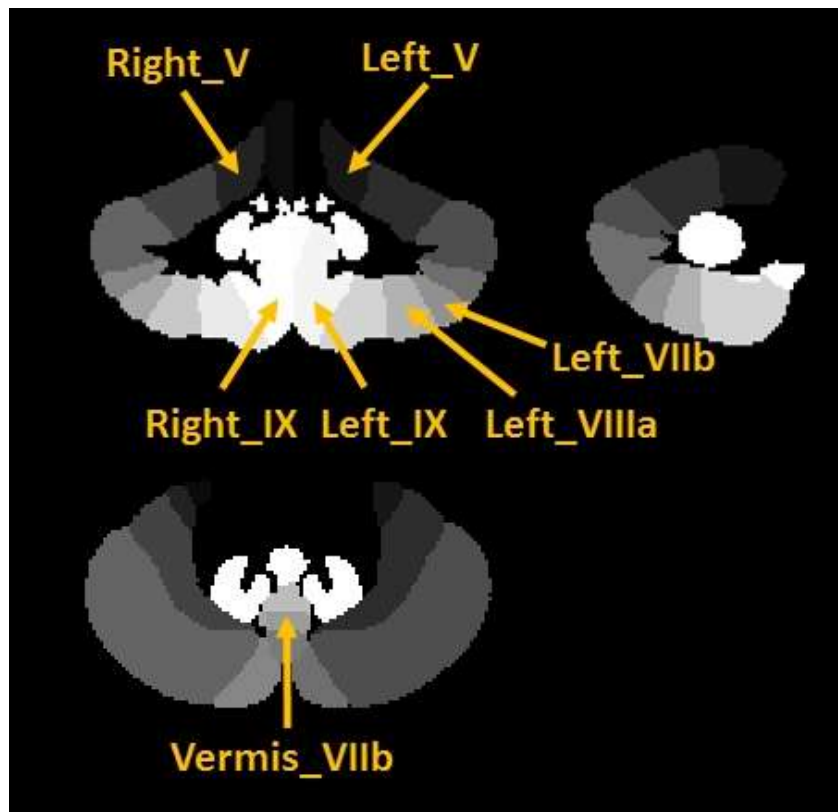


Figure 2.4 A cerebellar atlas from SUIT is shown labelled with representative regions that showed a significant loss in %GM between control subjects and subgroups of ET subjects. [Note that additional regions of significance could not be displayed given they are visible on different images.]

## 2.4 Discussion

In this study we showed that ET cases with various forms of cranial tremor differed from controls with respect to cerebellar GM, with evidence of GM reduction across several cerebellar regions. Our study is unique in the sense that it quantified %GM density in 34 distinct lobules of the cerebellum in cases and age-matched controls using high resolution 3D T1-Weighted MRI. We are aware of one other study that used a similar but not identical approach, namely, a voxel based morphometry study of 28 manually defined lobules of the cerebellum in 39 ET cases and 36 controls based on a cerebellar atlas from a single subject. In that study, a reduction in GM volume was noted in vermis lobules VI and VII, which are contiguous areas of the cerebellar

vermis (Shin et al., 2016). All other studies have treated the cerebellum as an entire organ, as two hemispheres or as anterior and posterior regions, but have not used a lobule by lobule approach (Choi et al., 2015; Lin et al., 2013). One partial exception is a study that examined 6 regions of the cerebellum (bilateral dentate and bilateral cerebellar lobules VI and VIII), noting that there was GM loss in lobule VIII (Gallea et al., 2015).

Voxel based morphometry studies identify clusters of change between two groups but do not specifically delineate boundaries of individual cerebellar lobules. Overlap of these clusters across lobular boundaries and contribution from each lobule is uncertain. Physiologically, cerebellar function may cross these lobular boundaries to include multiple lobules as shown in several fMRI studies in ET (Mayka, Corcos, Leurgans, & Vaillancourt, 2006; Sharifi et al., 2014). Typically, only the center of a statistically significant cluster in MNI or Talarach space is cross-referenced to a location within a published cerebellar atlas taken from a single subject (Schmahmann et al., 1999). A source of error in the resulting cerebellar lobule boundaries may also occur when non-linear normalization forces unique subject specific cerebellar architecture into a fixed template. Additionally, automated segmentation techniques such as FreeSurfer do not identify specific lobular boundaries of the cerebellum. Our study specifically utilizes a lobular probabilistic atlas of the cerebellum based on 20 subjects to identify regional %GM density change between subgroups.

In the current study, we detected a reduction in %GM density in ET cases, and more specifically, those with head and jaw tremor and voice tremor, across a range of cerebellar lobules. These changes in GM density could not be accounted for by variations in age, gender or MoCA score. We hypothesize that a decrease in %GM density between groups would represent atrophy in a specific cerebellar lobule. However, a decrease in %GM could also be accounted for

by an increase in % WM (Sharifi et al., 2014). Only one study found changes in both cerebellar GM and WM density in ET using a VBM analysis uncorrected for multiple comparisons (Benito-León et al., 2009).

One prior study examined 6 regions of the cerebellum (bilateral dentate and bilateral cerebellar lobules VI and VIII) and reported GM loss in lobule VIII among 19 ET cases vs. 19 controls (Gallea et al., 2015). The same authors, using functional MRI in 21 ET cases and 21 controls, performed a lobule by lobule analysis of the cerebellum, reporting tremor-related activations bilaterally in the cerebellum in left and right lobules V and VI and in right lobules VIIIa and VIIIb (Broersma et al., 2016). As noted by the authors, lobules V and VI have strong primary somatosensory representation and lobule VIIIb, a secondary representation. Our study confirmed decreases in %GM density in lobules V and VIII as well as additional regions found to be different in prior imaging studies of ET (Louis et al., 1998, 2016; Shin et al., 2016). We also report decreases in GM density in lobules I-IV, V, VI, VII and VIII as well as the vermis (Table 2.2). Additional work, using a lobule-by-lobule approach, is needed to confirm these results and precisely map the regional differences in ET cases, subgroups of ET cases, and controls.

Based on postmortem studies, a number of changes have been described in the ET cerebellum. Some though not all studies have noted the presence of Purkinje cell loss. Similarly, marked reductions in the Purkinje cell dendritic arbor have been noted in ET cases compared to controls; before degeneration, the metabolic economy of neurons is severely challenged, and they are unable to maintain their extensive cytoskeleton, and this can manifest as regressive changes in dendritic morphology (e.g., a truncation of the dendritic arbor) (Louis et al., 2014).

Studies such as ours and those mentioned above suggest that such cellular changes may be accompanied by reductions in GM density in ET cases in the cerebellum.

## **2.5 Conclusion**

Our results show that the presence of cranial tremor and voice tremor in ET may be manifested in a reduction in lobular cerebellar %GM density between groups independent of age, gender or MOCA score. Knowledge of MRI determined regional changes in this disease may add to information on the role of the cerebellum in ET. Identification of regions with the greatest degree of %GM density change compared to that in normal aging may also aid in identifying causative mechanisms and biomarkers of disease progression.

### **3. CEREBRAL GRAY MATTER VOLUME LOSSES IN ESSENTIAL TREMOR: A CASE-CONTROL STUDY USING HIGH RESOLUTION TISSUE PROBABILITY MAPS**

*Published in Parkinsonism and Related Disorders 51 (2018) 85-90*

*Eric Cameron, Jonathan P. Dyke, Nora Hernandez, Elan D. Louis, Ulrike Dydak*

#### **3.1 Introduction**

Essential tremor (ET) is among the most common movement disorders (Louis & Ottman, 2014). Tremor in the head and neck may occur in addition to arm tremor. The precise localization of the problem that results in tremor in ET is not known, but is thought to involve motor loops passing through the cerebellum, and there is even some evidence that the cerebellum itself may be the primary seat of the problem (Benito-León & Labiano-Fontcuberta, 2016; Cerasa & Quattrone, 2016; Filip, Lungu, Manto, & Bares, 2016). Hence, imaging studies in ET have focused particular attention on the cerebellum (Cerasa & Quattrone, 2016). While on the one hand investigators have been honing in on the cerebellum, there is greater and greater appreciation of the fact that ET seems to be a multi-dimensional disorder, with both motor and non-motor (e.g., cognitive) features (Louis, 2016), and studies of the cerebral cortex have become the subject of greater interest. Interestingly, imaging studies of subjects with spinocerebellar ataxia (SCA) similarly show that while there is an expected involvement of the cerebellum, the cerebral cortex is involved, pointing to a more diffuse form of degeneration (Dohlinger, Hauser, Borkert, Luft, & Schulz, 2008; Hernandez-Castillo, Galvez, Diaz, & Fernandez-Ruiz, 2016). On this basis, we hypothesized that (1) volume loss in ET would not be restricted to the cerebellum and (2) volume loss would involve areas in the cerebral cortex that are involved in movement.

One of the most important factors that introduces inconsistency between studies assessing brain volume loss is the multitude of anatomical segmentation algorithms used to classify the brains tissues. While many studies use the same software, SPM (<http://www.fil.ion.ucl.ac.uk/spm/>), the preprocessing steps have many variables that greatly affect the overall measure of tissues in the brain. Standard procedures are outlined by Ashburner and Friston (Ashburner & Friston, 2000), but there are more recent papers (Ashburner, 2009; Ashburner & Friston, 2005) that update preprocessing procedures to more accurately reflect improvements in the algorithms and image quality. Segmentation in SPM is performed using Bayesian probability and tissue probability maps (TPMs). The TPMs are morphed to the subject brain and used to create tissue maps for each subject. Thus, the quality of the TPMs will greatly affect the quality of the subject's tissue maps. The brain is segmented into three tissue types: gray matter (GM), white matter (WM), and cerebrospinal fluid (CSF). After segmentation, the subjects' brain images must be normalized to a common space, typically Montreal Neurologic Institute (MNI) space, using an atlas. This involves both linear and non-linear warping of the subject brain. An important step in normalization is the "modulation" of the image, which preserves the amount of a specific tissue type in each voxel (Ashburner, 2009). Finally, smoothing of the normalized tissue maps is necessary to ensure parametric statistics can be performed (Ashburner & Friston, 2000). In order to use parametric statistics to test for volume changes, a minimum of 30 degrees of freedom is recommended (Friston et al., 1995). Therefore, when working with a population of fewer than 30 subjects, using non-parametric statistics is recommended. The current study greatly exceeds that threshold, having 47 and 36 subjects in the case/control groups respectively, for a total of 83 subjects. This threshold is maintained in subgroup tests as well.

To date, seven studies (Table 2.1) (Bagepally et al., 2012; Benito-León et al., 2009; Bhalsing et al., 2014; Buijink et al., 2015; Daniels et al., 2006; Lin et al., 2013; Nicoletti et al., 2015) have investigated brain volume loss in ET, both in the cerebrum and cerebellum, although they are inconsistent across methods and results. The inconsistencies in results are likely due to the underutilization of the high-resolution 3D images that are required for segmentation. Using a set of TPMs with a lower resolution than the original image essentially down-samples the resulting tissue maps to the resolution of the TPMs. The same can be said about the smoothing kernels; too large of a smoothing kernel will effectively lower the resolution and waste the high resolution benefits. By sampling to the same resolution

Table 3.1 Chronological summary of VBM studies in essential tremor. A check mark indicates the attribute was included in the study. Abbreviations: Gray Matter (GM), ET with intention tremor (ET-I), ET with postural tremor (ET-P), control for ET-I (C-I), control for ET-P (C-P).

Authors	Main Result	3.0T MRI	1x1x1 mm <sup>3</sup> GM maps	≥ 30 subjects in every test	Multiple comparison correction	4 mm isotropic smoothing	High resolution atlas
Daniels et al. 2006	No GM changes were reported when comparing cases to controls. ET with intention tremor showed an increase in GM volume in the bilateral superior temporal gyrus compared to ET with postural tremor only. This test was performed with both ET groups compared to their respective controls (i.e. ET-I vs. C-I > ET-P vs C-P).						
Benito-Leon et al. 2009	Comparing cases and controls, GM change (direction not specified) was found in the bilateral parietal lobe, right frontal lobe, and right insula. Comparing ET with head tremor and controls, GM change was reported in the right parietal and temporal lobes.	✓		✓			
Bagepally et al. 2012	Comparing cases and controls, GM atrophy was found in the bilateral frontal and occipital lobes, left middle temporal gyrus, and right superior parietal lobe. Comparing ET with and without head tremor, GM atrophy was found in the bilateral temporal and frontal lobes, right parietal lobe, and insula.	✓	✓				
Lin et al. 2013	Comparing cases and controls, GM atrophy was reported in the caudate, left mid temporal pole, insula, left precuneus, and superior temporal gyrus. Also, an increase in GM volume was reported in the mid temporal pole and precentral gyrus.	✓					
Bhalsing et al. 2014	This study separated the cases into those with and without cognitive impairment. An ANOVA comparing these two groups with controls found GM atrophy in the left anterior cingulate, right precentral gyrus, right occipital lobe, left superior temporal gyrus, and right insula.	✓	✓	✓	✓		
Buijink et al. 2015	No GM changes were reported when comparing cases to controls. Comparing ET with and without head tremor, an increase in GM volume was reported in ET with head tremor in the bilateral pre-/post-central gyri, and left superior medial gyrus.		✓	✓	✓		
Nicoletti et al. 2015	No GM changes were reported when comparing cases to controls or when comparing subgroups of ET with and without resting tremor.	✓	✓	✓			
Cameron et al. 2017	When comparing cases to controls, GM volume loss is found in the posterior insula, superior temporal gyri, cingulate cortex, inferior frontal gyri and other occipital and parietal regions. Multiple subgroups including ET with head tremor and ET with severe tremor were compared against controls. An ANOVA between ET with and without head tremor and controls was performed as well.	✓	✓	✓	✓	✓	✓

as the original image, segmenting with TPMs of the same resolution as your 3D image, and smoothing by a smaller kernel, the high resolution of the original 3D image can improve the accuracy of the end result. Finally, correcting for multiple comparisons is essential when performing a voxel-wise analysis; however, identifying a correction procedure that minimizes both type I and type II errors is challenging.

This study aims to address these issues by utilizing the International Consortium for Brain Mapping (ICBM) 2009a high-resolution ( $1 \times 1 \times 1 \text{ mm}^3$ ) atlas and TPMs (Fonov et al., 2011; Fonov, Evans, McKinstry, Almlil, & Collins, 2009) for segmentation and normalization. Additionally, the parameters for preprocessing are carefully selected to optimize the detection of GM atrophy in the cerebrum. Cerebellar volume loss in this ET cohort has been reported previously (Dyke, Cameron, Hernandez, Dydak, & Louis, 2017).

## **3.2 Methods**

### **3.2.1 Clinical Assessment**

The study protocol was approved by the Yale, Cornell, and Purdue Human Subjects Institutional Review Boards. Written informed consent was obtained from each subject upon enrollment.

ET cases were recruited from a clinical-epidemiological case-control study of ET, from the neurological practice of one of the authors (E.D.L.), and via study advertisements (Dyke et al., 2017). Normal control subjects were recruited during the same time period and from the same sources as the ET cases, with some being spouses of the ET cases (Dyke et al., 2017). They were matched to ET cases on age. As cases were more readily available, their recruitment occurred more easily than those of controls, and this contributed to an unequal number of cases and controls (Dyke et al., 2017). Controls were excluded if they had history or family history of

ET (a first- or second-degree relative with ET). Inclusion criteria for ET was a diagnosis of ET from the treating neurologist and a willingness to undergo MRI. General exclusion criteria included heavy ethanol exposure (Harasymiw & Bean, 2001), a history of neurodegenerative disease (dementia, Parkinson's disease), prior deep brain stimulation or other neurosurgery, or contraindication for MRI.

Upon enrollment, each ET case had an in-person assessment by a trained research assistant to collect demographic and clinical data, including the Montreal Cognitive Assessment (MoCA) (score range 0 – 30) to briefly assess cognitive function and screen for mild cognitive impairment (MCI) (Nasreddine et al., 2005). Questionnaires collected data on a broad range of aging-related comorbidities (e.g., hearing loss, osteoarthritis, stroke) as well as years since most recent hospitalization and number of prescription medications, both of which also reflect burden of co-morbidity. Additionally, a video-taped neurological examination was performed on all subjects, which included 12 tests to assess postural and kinetic tremor. The video-tapes were reviewed by a neurologist specialized in tremors (E.D.L.) who scored each of 12 tests using the 0-3 Washington Heights-Inwood Genetic Study of Essential Tremor (WHIGET) rating scale (range of total tremor score [TTS] = 0 - 36). Head (i.e., neck) and jaw tremor were each scored as absent (0) or present (1). Diagnoses of ET were re-confirmed by the neurologist (E.D.L.) based on the history and videotaped neurological examination - WHIGET diagnostic criteria were applied (moderate or greater amplitude kinetic tremor [tremor rating  $\geq$  2]) during three or more tests or the presence of a head tremor, in the absence of Parkinson's disease, dystonia or another cause.

Table 3.2 Demographic and clinical characteristics. P-values are with respect to controls for each group. 9M/4F ET cases were included both in the ETH and ET-ST subgroups.

Abbreviations: ET with head tremor (ETH), ET with severe tremor [TTS $\geq$ 23] (ET-ST), Montreal Cognitive Assessment (MoCA), Not Applicable (N/A), Years since hospitalization (#Years Hospit), Number of prescription medications (# Prescrip), Transient Ischemic Attack (TIA), Congestive Heart Failure (CHF), Myocardial Infarction (MI), Osteoarthritis (OA)

	ET Cases	ETH	ET-ST	Controls
Sex	24M/23F (51% M) p = 0.033	13M/14F (48% M) p = 0.099	14M/7F (67% M) p = 0.004	10M/26F (28% M)
Age (years)	76.0 $\pm$ 6.8 p = 0.075	77.4 $\pm$ 6.9 p = 0.023	77.8 $\pm$ 6.6 p = 0.019	73.3 $\pm$ 6.5
Total Tremor Score	20.4 $\pm$ 6.1 p < 0.001	20.4 $\pm$ 6.3 p < 0.001	24.8 $\pm$ 1.8 p < 0.001	5.3 $\pm$ 2.5
MoCA Score	27.4 $\pm$ 2.5 p = 0.135	27.8 $\pm$ 1.9 p = 0.426	26.8 $\pm$ 3.0 p = 0.040	28.1 $\pm$ 1.7
Age of Onset (years)	41.0 $\pm$ 20.5	41.9 $\pm$ 20.8	36.0 $\pm$ 21.6	N/A
#Years Hospit	8.4 $\pm$ 13.3 p = 0.002	8.0 $\pm$ 10.2 p = 0.002	6.9 $\pm$ 6.9 p < 0.001	22.8 $\pm$ 23.9
#Prescrip	3.56 $\pm$ 2.48 p=0.575	3.93 $\pm$ 2.29 p=0.372	3.70 $\pm$ 3.00 p=0.641	3.19 $\pm$ 3.21
Hearing loss	12/47 (26%) p=0.068	8/27 (30%) p=0.045	5/21 (24%) p=0.132	3/36 (8%)
Stroke	2/47 (4%) p=0.216	1/27 (4%) p=0.248	2/21 (10%) p=0.064	0/36 (0%)
TIA	3/47 (6%) p=0.458	0/27 (0%) p=0.386	1/21 (5%) p=0.700	1/36 (3%)
CHF	5/47 (11%) p=0.187	2/27 (7%) p=0.405	2/21 (10%) p=0.284	1/36 (3%)
MI	1/47 (2%) p=0.381	0/27 (0%) p=N/A	1/21 (5%) p=0.190	0/36 (0%)
OA	13/47 (28%) p=0.626	7/27 (26%) p=0.766	5/21 (24%) p=0.904	8/36 (22%)

All MRI data was acquired at Weill Cornell Medicine at the Citigroup Biomedical Imaging Center on a 3 Tesla Siemens Tim Trio scanner (Siemens Healthcare, Erlangen, Germany) with a 32-channel head coil. For brain tissue segmentation, high resolution MPRAGE images were acquired (TR/TE/TI=2300/2.91/900ms, flip angle=9°, bandwidth:240 Hz/pixel, voxel size: 1.0mm×1.0mm×1.2mm, GRAPPA=2).

### **3.2.2 Data Processing**

This study utilizes the “Old Segment” and “Old Normalize” programs available in SPM12 for their ability to select different atlases and TPMs compared to the standard version. Although the newer versions have updated algorithms to accomplish the segmentation and normalization, the ability to select more accurate reference images is essential. To improve the segmentation and normalization, the updated ICBM 2009a atlas was used for normalization, and the included TPMs were used for segmentation. The atlas and the TPMs have a resolution of 1x1x1 mm<sup>3</sup>, matching the resolution of the subject images.

Each subject image was first manually aligned to the atlas using the Check Reg function in SPM12. Manual adjustment ensures a proper registration of the subject to the atlas during segmentation and greatly improves the likelihood of proper segmentation.

The batch “Old Segment” was run to segment the brain into three separate tissue classes; GM, WM, and CSF, with the TPMs included in the ICBM 2009a atlas. Each image was checked for proper anatomical segmentation by overlaying the resulting tissue maps onto the original T1-weighted image. Those that did not pass a visual inspection were manually realigned to the atlas and segmented a second time. Often segmentation will fail if the image to be segmented is too far out of alignment with the atlas. This can be remedied by simply translating and rotating the image, contoured over the atlas, until it visually matches the atlas.

Normalization was performed using the “Old Normalize” function where the original T1-weighted image was normalized to the ICBM 2009a atlas and the subsequent transformation applied to the T1-weighted image and the three tissue maps from segmentation. Additionally, the tissue maps were modulated to preserve the amount of tissue in each voxel. This changes the intensity (which corresponds to percent tissue) in each voxel proportional to how much the volume of that voxel changes during the applied transformation. The tissue maps were resampled to  $1 \times 1 \times 1 \text{ mm}^3$  resolution after transformation to retain the original resolution of the image and atlas.

Finally, the tissue maps were smoothed with a  $4 \times 4 \times 4 \text{ mm}^3$  FWHM kernel. This smoothing kernel is smaller than that used in previous studies (which mostly used an  $8 \times 8 \times 8 \text{ mm}^3$  FWHM kernel), but follows the guidelines that the smoothing kernel should be at least twice the voxel size (Friston, Holmes, Poline, Price, & Frith, 1996). There is a trade-off between detection efficiency and noise when considering the size of smoothing kernel. By increasing the size of the smoothing kernel, the signal-to-noise ratio (SNR) of the image is increased at the expense of image resolution, which in turn lowers detection efficiency (Friston et al., 1996). Therefore, due to overall better SNR from MRI images compared to earlier studies, and the improved segmentation with a high-resolution atlas, the images were smoothed by a reduced kernel.

### **3.2.3 Statistical Analysis**

All analyses were performed using the factorial design specification function in SPM12, which performs statistical comparisons on a voxel-wise level. Demographics, clinical features, and associated comorbidities of ET cases and controls were compared using Student's  $t$  and  $\chi^2$  tests. A two-sample  $t$ -test was used to test group differences with nuisance variables age, sex, and MoCA score. Intracranial volume was calculated as the sum of the three tissue maps (GM,

WM, and CSF) and included as a global calculation factor. Comparisons were performed for ET vs. Controls, ET with head or jaw tremor (ETH) vs. Controls, and ET with severe tremor (ET-ST) (i.e., total tremor score (TTS) $\geq$ 23, which required a rating of 3 [severe] on at least one item) vs. Controls. ETH and ET-ST were not mutually exclusive categories, as it was possible for an ET case to present both with head tremor and a TTS $\geq$ 23. Additionally, an ANOVA was performed to compare ET with and without head or jaw tremor and controls. A peak (voxel-wise) threshold was set at  $p < 0.001$  with a correction for multiple comparison using a cluster corrected  $p$ -value  $< 0.05$ . The cluster correction requires a certain number of significant voxels be connected (clustered) in order to be deemed statistically significant. The size threshold for a cluster to be deemed significant (cluster  $p$ -value set to  $p < 0.05$ ) is dependent on the voxel size, smoothing kernel, and other variables (Friston et al., 1995, 1994).

### **3.3 Method Validation**

#### **3.3.1 Smoothing Kernel**

To implement the high-resolution atlas into the SPM processing methods, a few parameters had to be optimized and validated against established methods. First, the “Old Segment” and “Old Normalize” routines were chosen due to their ability to select different probability maps and atlases compared to the newer versions. Also, due to the 8-fold increase in resolution, a decreased smoothing kernel is desired to take advantage of the higher resolution images.

The smoothing kernel should be double the voxel size, at a minimum, in order for certain mathematical assumptions to hold valid (Friston et al., 1996). Therefore, we compared three different smoothing kernels: 8 mm FWHM, 4 mm FWHM, and 2 mm FWHM (all isotropic). These values were chosen for the following reasons: 8 mm is the standard (default) smoothing kernel recommended in SPM. 4 mm FWHM would provide the same smoothing ratio compared

to the resolution of the tissue maps. For example, the default setting is to smooth 2 mm isotropic maps with an 8 mm FWHM isotropic kernel (smoothing ratio =  $512 \text{ mm}^3/8 \text{ mm}^3 = 64$ ). This ratio would remain the same smoothing 1 mm isotropic maps with a 4 mm FWHM isotropic kernel (smoothing ratio =  $64 \text{ mm}^3/1 \text{ mm}^3 = 64$ ). Finally, a 2 mm FWHM kernel is the minimum smoothing kernel recommended to allow the mathematical assumptions to hold true given a 1 mm isotropic tissue map.

All other processing steps were kept constant for these three trials. The smoothing tests were performed on a subset of ET with head tremor (24) and controls (25) from the ET study. This subset was used because the study had not finished collecting subject data when we began optimizing this method. The three kernels were compared based on the necessary size of voxel clusters to be deemed significant and the biological relevance of those cluster sizes. Additionally, we kept in mind that as the significant cluster size decreases, the possibility of false positives increases. The ideal significant cluster size is one that is biologically plausible to identify volume loss, but not so small that false positives become likely. We did not judge the best smoothing kernel based off of regions of significance, but there was little difference in significant regions because the subject set was kept constant for each smoothing kernel.

The 8 mm isotropic kernel was unnecessarily high, as seen by the significant cluster size being greater than 1000 voxels. Although it is not providing any incorrect results, the specificity of this size of smoothing kernel is poor given the high resolution of the tissue maps. Essentially it is a waste of the gained specificity of using such high resolution images. The 4 mm isotropic kernel had a significant cluster size of 181 voxels. Considering an isotropic voxel size of  $1 \text{ mm}^3$ , this cluster corresponds to a  $0.181 \text{ cm}^3$  affected volume (not lost volume), which is a much more reasonable size. Biologically, we would expect measureable GM volume loss (via imaging

methods) to be occurring on a macroscopic scale (in this case around  $0.181 \text{ cm}^3$  at a minimum). That is not to say a complete loss of  $0.181 \text{ cm}^3$  of brain volume, but rather a region of the brain larger than  $0.181 \text{ cm}^3$  has significant reduction in volume between groups. The 2 mm isotropic kernel had a significant cluster size of 54 voxels, which is minimally acceptable. However, when performing millions of statistical comparisons (one comparison per voxel), there will be many false positive results. While these false positives are mostly corrected for using the cluster thresholding, a lower threshold makes it more likely that a significant cluster is composed of false positive voxels. For this reason, the 4 mm kernel was chosen for this study as the ideal smoothing kernel. Additionally, the macroscopic structures of the brain are more on the same scale as the significant cluster size (181 voxels) from the 4 mm kernel. Ideally, we should be smoothing our images to the same scale as the regions of change we wish to detect, which is accomplished with the 4 mm isotropic kernel.

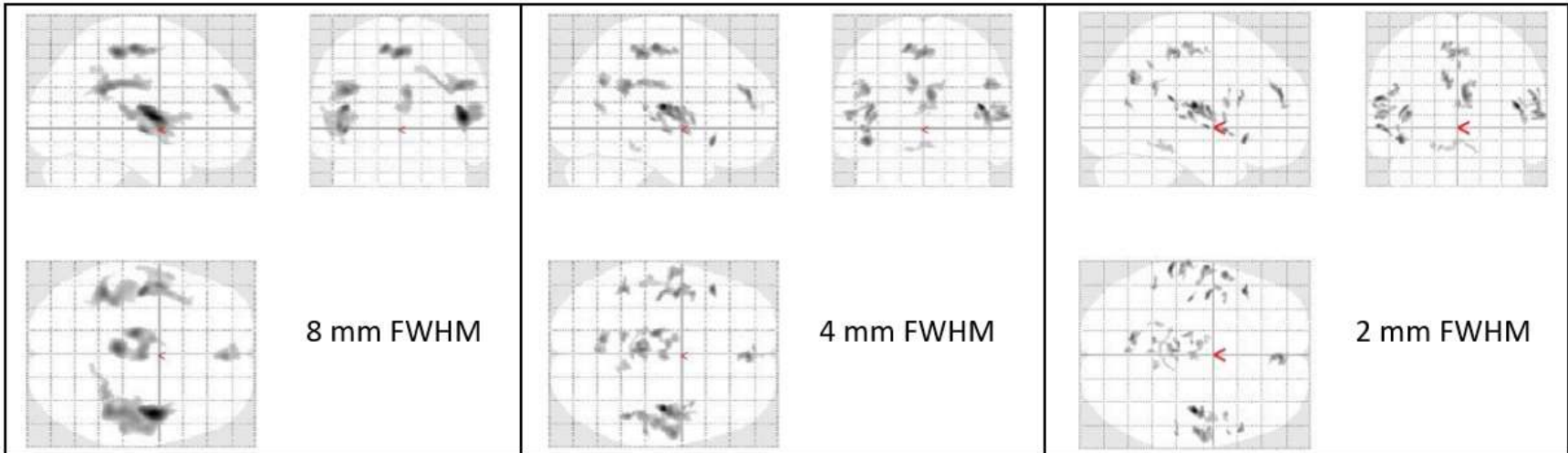


Figure 3.1 'Glass brain' view from SPM comparing significant clusters using three different smoothing kernels: 8 mm, 4, mm, and 2 mm. Clusters of the 4 mm smoothing kernel are closest in size to the biological change we expect.

### 3.3.2 Method Comparison

Having established an optimal smoothing kernel and processing method with the high resolution atlas, we wished to validate this method against the default processing methods in SPM. Our optimized method, named ‘adjusted’, used the “Old Segment” and “Old Normalize” algorithms with the high resolution ICMB 2009a atlas and TPMs and a smoothing kernel of 4 mm FWHM. This was compared against two other processing methods. The first was named ‘default’ and used the same “Old Segment” and “Old Normalize” algorithms with all settings unadjusted, and using the 2 mm isotropic MNI 152 atlas and TPMs included with SPM. The standard smoothing kernel of 8 mm FWHM was also applied. The second was named ‘DARTEL’ and this method follows the recommended steps outlined in the SPM manual to use the newest versions of segment, DARTEL, and normalize (Ashburner, 2010). This method uses the 1.5 mm isotropic MNI 152 atlas and TPMs included with SPM and a smoothing kernel of 8 mm FWHM.

These three methods were performed independently on the same group of 27 ET with head tremor and 36 controls. Whole brain voxel-wise results were compared based on multiple factors, including symmetry of results (biologically expected) and a lack of clusters in cerebellum and brainstem. VBM is not optimized for detecting changes in GM volume in the cerebellum due to the intricacy of the cerebellar cortex. A much higher resolution (at least 0.5 mm isotropic) would be necessary to accurately and confidently segment cerebellar GM and WM. As for the brain stem, it is not identified as either GM or WM, but rather a mixture of both. Therefore, any volume change could not confidently be identified as GM loss, nor would it likely be on a macroscopic scale as measureable with these methods. Due to these factors, significant clusters in the cerebellum and brain stem are thought to be false positives.

The same statistical method was used for each of the three tests, with extent cluster thresholding used to correct for multiple comparisons. The adjusted method showed mostly bilateral results, all confined to the cerebrum, while the default method showed only a few bilateral results, with a large number of clusters in the cerebellum and brainstem. The DARTEL method showed no significant clusters. Moreover, in the DARTEL method without multiple comparison correction, there were more clusters of increased GM volume than decreased GM volume in the cases compared to controls randomly dispersed throughout the brain. This indicates a systematic error, as regardless of multiple comparison correction, we should not be seeing wide spread volume *increase* in any group, especially in cases compared to controls.

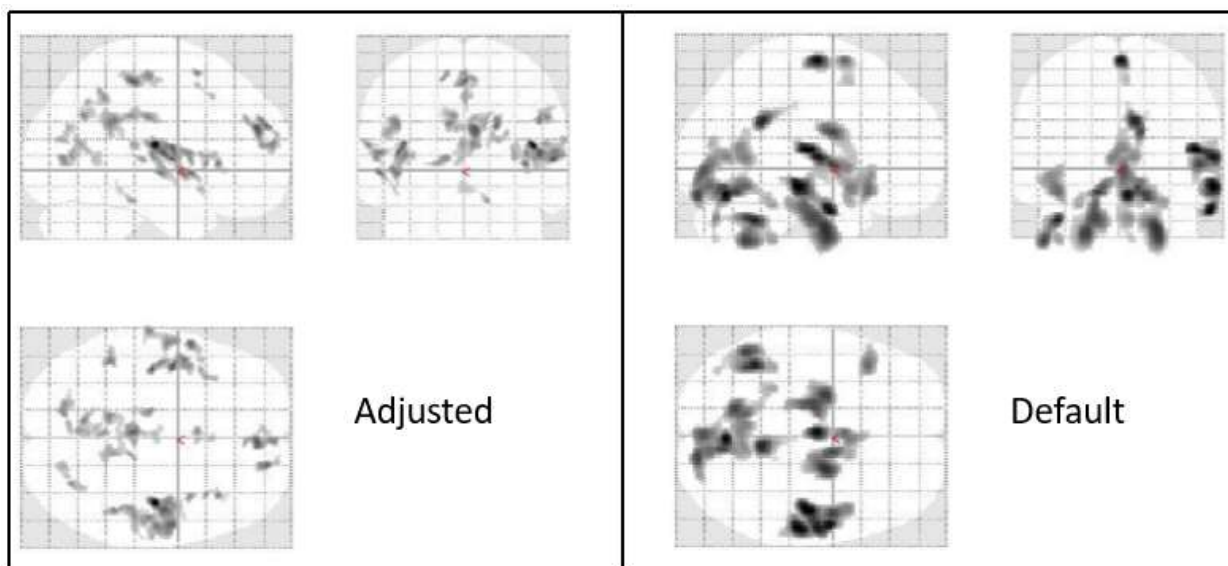


Figure 3.2 ‘Glass brain’ view of adjusted and default method results. Gray spots are clusters of significant voxels deemed significant on a cluster-wise level. Note the lack of clusters in the cerebellum and brainstem in the adjusted results compared to the default. DARTEL results showed no significant clusters after multiple comparison correction and are not displayed.

Based on the lack of significant clusters in the cerebellum and brainstem in the adjusted method, we feel confident that this method is more accurate compared to the default and DARTEL methods. Additionally, it is clear that the use of a higher resolution atlas and optimized

smoothing kernel has a large effect on the detectability and accuracy of GM volume loss using these methods. Not only is the distribution of GM volume loss more bilateral, but also the significant clusters are smaller and more accurately identify affected brain regions.

### 3.4 Results

ET and controls differed with respect to sex ( $p=0.033$ ) and years since most recent hospitalization ( $p=0.002$ ). Differences in age, MoCA score, and hearing loss ( $p=0.076$ ,  $p=0.135$ , and  $p=0.068$  respectively) were marginally significant (Table 3.2). Age, sex, and MoCA score were used as covariates in all statistical tests to factor out any possible confounding effects.

Statistically significant cerebral GM volume loss (cluster corrected  $p$ -value $<0.05$ ) was found widespread throughout the temporal, parietal, frontal and occipital lobes in ET vs C, ETH vs C and in the ANOVA (Table 3.3). The regions of highest significance were the Heschl, inferior insula, and superior temporal gyri, which had cluster corrected  $p$ -values $\leq 0.001$ . ETH vs C comparison and ANOVA showed the most widespread cerebral GM volume loss involving additional regions such as the anterior, middle, and posterior cingulate. Fewer regions were found to show statistically significant GM volume loss in the ET-ST vs C group comparisons, such as the right superior temporal gyrus, right rolandic operculum, right supramarginal gyrus, right precuneus, and right superior occipital lobe. Importantly, no regions of cerebral GM volume *increase* in ET cases were detected in any comparisons. Figure 3.1 presents the statistically significant clusters overlaid on an axial slice of the 3D T1 atlas used for normalization. In additional analyses, we included hearing loss and years since most recent hospitalization as additional covariates in our adjusted models; results did not differ (data not shown).

Table 3.3 Summary of statistically significant regions of GM volume loss in each test. Presented p-values are on the cluster level and are deemed statistically significant using a peak-voxel p-value  $< 0.001$  and a cluster corrected threshold at the cluster level of  $p < 0.05$ . The regional specificity of the cluster is defined by one or more “peak” voxels in the cluster. Therefore, it is possible for a single cluster to belong to multiple brain regions in close proximity. Peak voxels are presented in SPM with a set of MNI coordinates that can be checked on the Automated Anatomical Labeling (AAL) atlas. ANOVA compared three groups: ET with head tremor, ET without head tremor and controls. Abbreviations: “vs” refers to a group comparison between two subject groups. Essential tremor (ET), Control (C), ET with head tremor (ETH), ET with severe tremor [TTS  $\geq 23$ ] (ET-ST). Right side (R), left side (L). Analysis of Variance (ANOVA).

Brain Region	ET vs C	ETH vs C	ET-ST vs C	ANOVA
<b>Temporal Lobe</b>				
R Heschl	<0.001	<0.001		<0.001
L Heschl	0.003			
R Insula	<0.001	<0.001		<0.001
L Insula		0.027		0.008
R Sup Temporal	<0.001	<0.001		
L Sup Temporal	0.003	<0.001	0.014	
R Rolandic Oper			0.014	
L Rolandic Oper		<0.001		0.008
<b>Parietal Lobe</b>				
R Supramarginal	0.033	<0.001	<0.001	
L Supramarginal		0.002		0.028
R Post Cingulate	0.006	0.001		
L Post Cingulate	0.037	0.003		0.042
R Paracentral lobule				0.019
L Paracentral lobule		<0.001		0.019
R Mid Cingulate		0.016		
<b>Frontal Lobe</b>				
R Supp Motor area		0.016		
L Supp Motor area		<0.001		
R Frontal Sup		0.007		0.016
R Frontal Sup Medial	0.001	<0.001		0.001
R Ant Cingulate	0.001	<0.001		0.001
<b>Occipital Lobe</b>				
R Calcarine		0.018		
L Calcarine	0.026	<0.001		0.022
R Precuneus	0.006		0.015	
L Precuneus	0.037	0.011		0.032
R Sup Occipital			0.047	
L Mid Occipital		0.011		
L Cuneus		<0.001		0.022

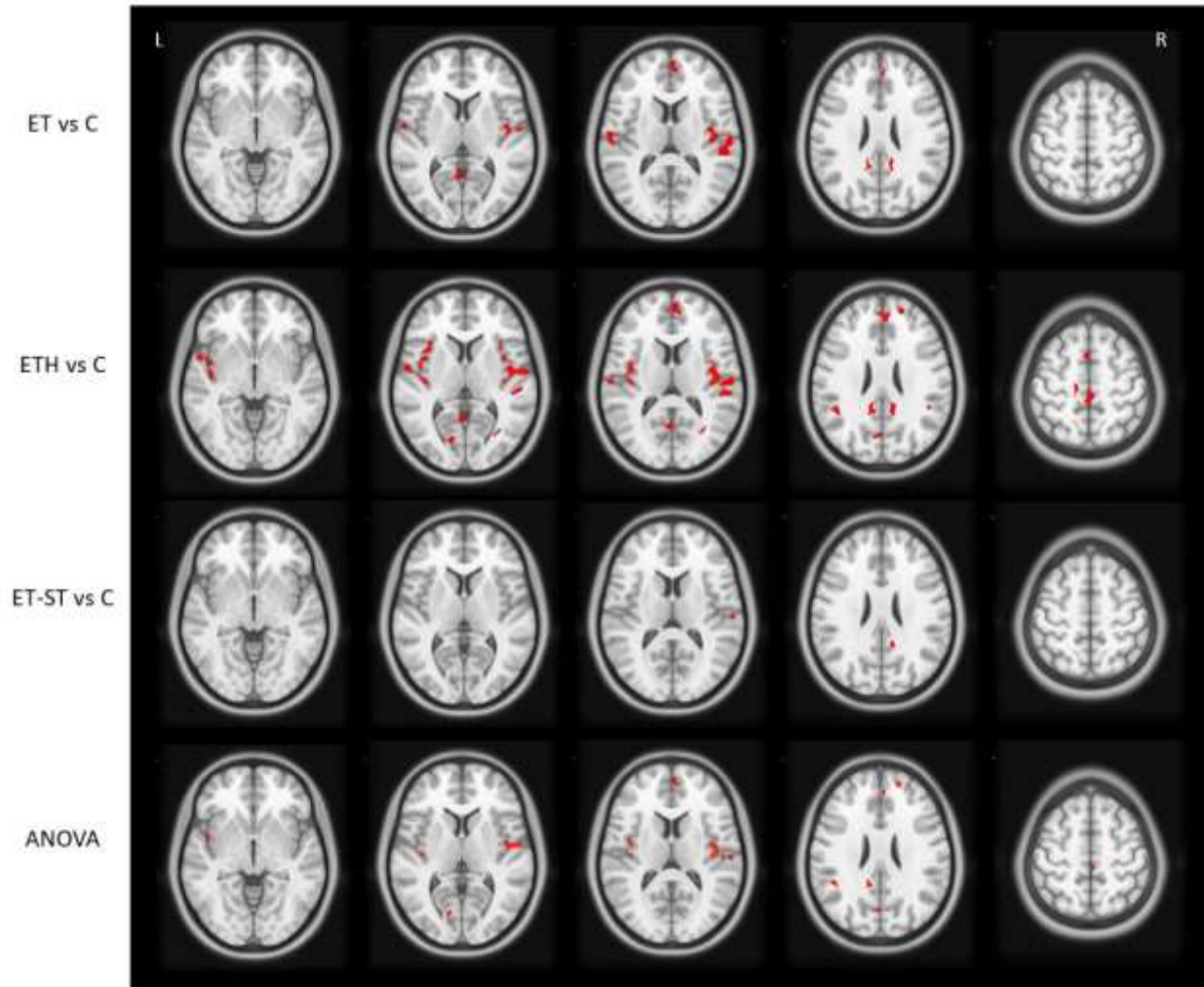


Figure 3.3 Axial slice view of statistically significant clusters (in red). Statistical significance is determined using a peak-voxel  $p$ -value  $< 0.001$  and a cluster corrected threshold at the cluster level of  $p < 0.05$ . ANOVA was run with three groups: ET with head tremor, ET without head tremor and controls. Abbreviations: “vs” refers to a group comparison between two subject groups. Essential Tremor (ET), Control (C), ET with head tremor (ETH), ET with total tremor score  $\geq 23$  (ET-ST), Analysis of Variance (ANOVA).

### 3.5 Discussion

We investigated cerebral GM volume loss in phenotypic subgroups of ET and in the ET group as a whole compared to controls. Previous studies have used SPM to investigate cerebral GM volume changes in ET populations and many have conducted subgroup analyses as well (Bagepally et al., 2012; Benito-León et al., 2009; Bhalsing et al., 2014; Buijink et al., 2015; Daniels et al., 2006; Lin et al., 2013). To our knowledge, however, this is the first study to

investigate cerebral GM volume loss in ET using the high-resolution ICBM 2009a atlas and TPMs for segmentation and normalization.

Although GM volume loss can be a feature of aging, it is important to emphasize that our study accounted for the effects of age and aging. First, we enrolled an age-matched control group, thereby allowing us to demonstrate changes in ET that were above and beyond those seen in normal aging. Second, we included age as a covariate in all statistical analyses; thus differences between ET groups and controls were completely independent of the effects of age. We also considered a broad range of aging-associated comorbidities, the vast majority of which did not differ between ET and controls, and for those that did (years since most recent hospitalization and hearing loss, marginally), adjustment in our models revealed that they did not influence our results.

By utilizing the high-resolution atlas and TPMs, this study was able to consistently identify regions of GM volume loss in ET and in ET subgroups. Regions such as the Heschl region, posterior insula, and superior temporal lobe were previously reported (Bhalsing et al., 2014; Daniels et al., 2006; Lin et al., 2013), however, we now report more widespread differences throughout the cerebrum as well. In addition to the regions noted above, significant GM volume loss was noted in the anterior, middle, and posterior cingulate, right frontal superior medial lobule, and occipital regions such as the calcarine, precuneus and cuneus. This study points clearly to the fact that volume loss is not restricted solely to the cerebellum in ET. Of additional note is that we found no statistically significant increases in GM volume in any of our case groups compared to controls, as have been previously reported (Buijink et al., 2015; Daniels et al., 2006; Lin et al., 2013). The consistency of results between the ET vs C, ETH vs C, and

ANOVA comparisons speaks to the improved detectability of GM volume loss using the high-resolution atlas.

Regions of significant difference between ET-ST and controls were less widespread than between ETH and controls. It is possible that sample size played a role ( $n = 21$  for ET-ST vs.  $n = 27$  for ETH). It is also possible that ETH represents a bone fide disease subtype (i.e., a “trait” difference) whereas ET-ST, merely a reflection of duration of tremor (i.e., a “state” difference). Indeed, other studies have consistently pointed to head tremor as a separable group of ET cases.

As noted above, this study suggests that volume loss is not restricted solely to the cerebellum in ET. Similarly, studies of patients with diseases characterized by more marked cerebellar involvement (e.g., SCA) indicate the presence of volume loss in the cerebral cortex as well (Dohlinger et al., 2008; Hernandez-Castillo et al., 2016), indicating a more diffuse degeneration.

One limitation of some studies is population size. It is recommended to have a minimum of 30 degrees of freedom (i.e. 30 subjects) when performing parametric statistics to test for GM volume differences between groups (Friston et al., 1995). Three prior studies (Table 3.1) (Bagepally et al., 2012; Daniels et al., 2006; Lin et al., 2013) performed group or subgroup tests that violated this threshold. This study was well above the threshold with a total of 83 subjects, with more than 30 in the control group, therefore the use of parametric statistics was validated for each test.

Functional and diffusion-based connectivity studies on healthy volunteers (Cauda et al., 2011; Jakab, Molnár, Bogner, Béres, & Berényi, 2012) have shown connections between the posterior insula and many of the regions this study reports as having statistically significant GM

volume loss. The posterior insula is the most consistent finding among our subgroup comparisons, indicating that this could be one of the first regions in the cerebrum to be affected by GM volume loss in ET. Diffusion tractography showed structural connectivity between the posterior insula and multiple regions in the cingulate cortex and somatosensory regions such as the supplementary motor cortex, which showed GM volume loss in our ETH comparison (Jakab et al., 2012). Similar results are presented in a functional connectivity study on healthy volunteers (Cauda et al., 2011), where the posterior insula is connected to the cerebellum as well as the posterior cingulate, sensorimotor, premotor, supplementary motor, and temporal cortices. Many, but not all, of these regions were found to have statistically significant GM volume loss in this study. This promotes the hypothesis that GM volume loss follows the motor paths from the cerebellum (see (Dyke et al., 2017)) up into the insula and continues along the associated motor pathways.

Several prior studies (Cerasa et al., 2009; Choi et al., 2015; Daniels et al., 2006; Nicoletti et al., 2015; Quattrone et al., 2008) have reported no GM volume change in the cerebrum when comparing ET cases and controls. We have shown that GM volume loss can be observed in the ET population as a whole, and that it is even more prevalent in ET with head tremor. The null results in the prior studies are likely a byproduct of lower resolution tissue maps.

We did not investigate regional correlations of GM volume and cognitive variables as this would have required a lobule approach to segmentation. Furthermore, the use of the MoCA in place of a full neuropsychological test battery was a limitation. While MoCA score was factored into each statistical test, it is not a fully reliable score that could be used to compare GM volume loss between groups of differing cognitive function. Another limitation of this study was that all subjects remained on prescribed medication for the exam and MRI. Tremor medication is

well-known to affect cognitive function, but it is not associated with cortical atrophy, so it was not considered necessary to withhold medication in the current study.

### **3.6 Conclusions**

This study provides evidence that GM volume loss in ET is present beyond the cerebellum, and in fact, is widespread throughout the cerebrum as well. Further, head tremor in ET has been shown to potentially be a subtype of the disease, with a propensity towards greater GM volume loss in the cerebrum, specifically in the posterior insula and its functionally connected regions. The consistency between comparisons validates the use of an updated and improved atlas for use in VBM. The depth and complexity of such analysis requires careful consideration of each step in the processing. Comparison of regional cerebral GM volume loss in ET may serve to provide information on disease progression and further identify subtypes of disease.

## **4. T2\* MRI PRESENTS DIFFERENCES IN IRON DEPOSITION IN ESSENTIAL TREMOR AND PARKINSON'S DISEASE**

### **4.1 Introduction**

Essential Tremor (ET) and Parkinson's Disease (PD) are both common movement disorders that present with similar symptoms and pathology, especially in the early onset of the disease state. Understanding the different neuropathology is essential for the differentiation and correct clinical diagnosis of these diseases. One important pathological feature of PD has been the increase of iron deposition in various brain regions. These iron deposits, specifically in the substantia nigra (SN), has been investigated for decades (Castellani, Siedlak, Perry, & Smith, 2000; Dexter et al., 1987; Dexter et al., 1991; He et al., 2015; Homayoon et al., 2018; Langkammer et al., 2016; Ulla et al., 2013; Ward et al., 2014; Zecca et al., 2004). It is well established however, that iron accumulates in the Lewy bodies present in the SN in PD (Castellani et al., 2000), in addition to the oligodendrocytes, microglia, and neurons (Zecca et al., 2004). Few studies, however, have investigated iron deposition in the brain in ET.

Magnetic resonance imaging (MRI) quantitative methods such as T2\* and Quantitative Susceptibility Mapping (QSM) have made detecting brain iron non-invasive and more reliable in-vivo. Specifically, T2\* mapping is a quantitative measure of the effect of magnetic field inhomogeneity on the transverse relaxation rate. These inhomogeneities occur due to multiple factors, some having only microscopic effects (Chavhan, Babyn, Thomas, Shroff, & Haacke, 2009). Iron, being a strongly paramagnetic material in tissue, causes microscopic inhomogeneities that can be quantified with T2\* mapping to determine a relative concentration of local iron.

One study (Novellino et al., 2013) has investigated iron deposition in ET with T2\* using a whole brain, voxel based approach. However, T2\* imaging parameters beyond the use of 16 echo times were not reported. They report a bilateral increase in iron deposition in the globus pallidus (GP), SN, and in the right dentate. After correction for multiple comparisons, only the bilateral GP remained significant however. Another study (Homayoon et al., 2018) investigated iron deposition with R2\* mapping in multiple movement disorders, including PD, tremor in dystonia (TiD), and ET. This study reports a significant increase in R2\* signal in the SN, synonymous with an increase in iron, in PD compared individually to the other three groups (two disease groups and controls). Further, no significant difference between ET and controls is reported in the SN. Finally, this study reports no significant difference in R2\* signal in the GP between any of the four groups, although there was a non-significant trend between ET and control. Further investigation into iron deposition in the SN and GP in ET is necessary to determine if there is a change in local iron.

Multiple studies have investigated iron deposition in PD using quantitative imaging methods (He et al., 2015; Homayoon et al., 2018; Langkammer et al., 2016; Ulla et al., 2013), with increased iron in the SN being the most common finding. Although no significant differences are reported in these studies in the GP, this region is of interest due to its direct involvement in tremor pathology for both diseases (Helmich, Toni, Deuschl, & Bloem, 2013). Furthermore, the GP is one of the primary regions of focus in the case of Manganese (Mn) toxicity. Excessive exposure to Mn can lead to the development of Manganism, a parkinsonian type disorder, with Mn accumulating most notably in the GP in addition to other brain regions. While there are certain distinctions between Manganism and PD, the alteration of the nigrostriatal dopaminergic pathways in the GP are shared between both disorders (Aschner,

Erikson, Hernández, & Tjalkens, 2009). Therefore, the SN and GP are of primary interest in the study of iron accumulation due to disease states.

The role of iron in the neurodegenerative process is still not fully understood, but it is thought that excess iron can locally initiate oxidative stress. Castellani et al. (2000) investigated whether iron present in the Lewy body formations in the SN contained iron in a suitable form for the Fenton reaction to occur. In the Fenton reaction, hydroxyl free radicals are formed that cause oxidative stress, which has been shown to lead to neurodegeneration. Indeed, they report redox-active iron in the Lewy bodies in the SN but not in cortical Lewy bodies. This is an important distinction between PD and ET, because ET cases typically do not present with Lewy body formations in the SN (Louis et al., 2007).

To further complicate matters, iron deposition in the brain has been shown repeatedly to increase with age (Acosta-Cabronero, Betts, Cardenas-Blanco, Yang, & Nestor, 2016; Ward et al., 2014; Zecca et al., 2004). Iron is an essential element for healthy brain metabolism and concentrates in the oligodendrocytes and astrocytes in normal iron homeostasis. Multiple mechanisms are thought to be responsible for the accumulation of iron in certain brain regions with aging, such as compromised iron homeostasis, inflammation, and increased blood-brain barrier permeability. This accumulation of iron is not uniform throughout the brain, but rather concentrates in specific regions, with the SN and GP being among the affected regions (Ward et al., 2014). This result has been reproduced in quantitative imaging studies using both ROI and whole brain approaches (Acosta-Cabronero et al., 2016). Given these findings, it is important to consider the age distribution of the study population when investigating iron deposition in the brain.

This study investigated iron deposition in a cohort of ET cases and controls using MRI T2\* imaging. Additionally, two separate PD studies (cases and controls) with similar T2\* data were analyzed to serve as positive control examples. Direct statistical comparisons between studies was not performed, as each study used its own acquisition protocol and data was acquired on different scanners. Regardless, changes in iron deposition in the SN in PD should be observable irrespective of mild sequence or scanner differences. This study aims to validate this point with our two separate PD cohorts. Further, we aim to reproduce the lack of difference in iron deposition seen between ET cases and controls in the SN and GP.

## **4.2 Methods**

### **4.2.1 ET Study**

The ET subjects are from a larger study applying advanced neuroimaging to study ET (Cameron, Dyke, Hernandez, Louis, & Dydak, 2018), where T2\* images were acquired on 21 cases (age  $78.1 \pm 6.6$  years) and 27 controls. However, due to an uneven distribution of demographics in the control group, 12 age and sex matched controls (age  $77.7 \pm 5.5$  years) were selected prior to data analysis to serve as the control group (see Table 4.1). This study was approved by the Yale, Cornell, and Purdue Human Subjects Institutional Review Boards and written informed consent was obtained from each subject upon enrollment.

ET cases were recruited from a clinical-epidemiological case-control study of ET, from the neurological practice of one of the authors (E.D.L.), and via study advertisements. Normal age-matched control subjects were recruited at the same time and from the same sources as the ET cases, with some being spouses of the ET cases. Controls were excluded if they had history or family history of ET (a first- or second-degree relative with ET). Inclusion criteria for ET was a diagnosis of ET from the treating neurologist and a willingness to undergo MRI. General

exclusion criteria included heavy ethanol exposure (Harasymiw & Bean, 2001), a history of neurodegenerative disease (dementia, Parkinson's disease), prior deep brain stimulation or other neurosurgery, or contraindication for MRI (Cameron et al., 2018).

T2\* images were acquired on a Siemens 3T Prisma scanner with a 32 channel Siemens head coil using a gradient echo T2\* sequence (TR=1100 ms; TE = 3.7, 11.3, 18.5, 25.6, 32.7, 39.9 ms; flip angle = 60°; 0.625x0.625x5 mm; BW = 260 Hz/px; GRAPPA = 2). T2\* maps were generated on the Siemens workstation.

#### **4.2.2 PD Study 1**

PD study 1 subjects were recruited within a study primarily focused on how regular exercise benefits whole-body metabolism and other molecular and functional endpoints in PD and mild cognitive impairment (MCI), with multiple neuroimaging biomarkers for analysis including T2\* (Heckova et al., 2017; Krumpolec et al., 2017). In this study, T2\* data was acquired on 10 PD cases (age  $60.1 \pm 6.2$  years) and 7 age-matched controls (age  $64.7 \pm 7.8$  years) (see Table 4.1). Subjects were recruited through collaboration with neurologists and centers for individuals with memory impairment. Only early-stage PD cases (stages 1-3 on the Hoehn and Yahr scale, or those who were physically independent) were included. Exclusion criteria were severe chronic medical conditions, history of brain injury, liver and kidney dysfunction, neurologic disorders (other than PD), psychiatric illnesses, or metal implants. This study was approved by the respective Institutional Review Board, and written informed consent was obtained from each subject upon enrollment (Heckova et al., 2017).

T2\* images were acquired on a Siemens 3T Trio scanner with a 32 channel Siemens head coil using a T2\* gradient echo sequence (TR = 47 ms; TE = 3.4, 6.9, 10.4, 13.8, 17.3, 20.8, 24.5,

28.0, 31.5, 35.0, 38.5, 42.0; flip angle =  $14^\circ$ ;  $1.1 \times 1.1 \times 1.1$  mm; BW = 300 Hz/px; GRAPPA = 2). T2\* maps were generated on the Siemens workstation.

### 4.2.3 PD Study 2

PD study 2 subjects are from a study primarily focused on gamma aminobutyric acid (GABA) in PD, where T2\* images were also acquired for later use. This study recruited 21 cases with mild-moderate PD (age  $63.4 \pm 8.8$  years) and 18 age-matched controls ( $58.9 \pm 10.3$  years) to participate in the study (see Table 4.1) (Dydak, Dharmadhikari, Snyder, & Zauber, 2015). 3 PD cases were medication-naïve (never taken Parkinson's medication); all other cases were off medication at least 12 hours prior to their scan. Exclusion criteria were any history of neurological disorder, dementia, severe rest tremor, claustrophobia, or current daily use of any GABA-ergic drugs (such as gabapentin and benzodiazapines). The study was approved by the Indiana University Institutional Review Board and written informed consent was obtained prior to participation from all subjects.

T2\* images were acquired on a Siemens 3T Trio scanner with a 32 channel Siemens head coil using a T2\* gradient echo sequence (TR= 800ms; TE = 4.4, 11.6, 19.4, 27.0, 34.5 ms; flip angle =  $20^\circ$ ;  $1 \times 1 \times 2$  mm; BW = 300 Hz/px; GRAPPA = 2). T2\* maps were generated on the Siemens workstation.

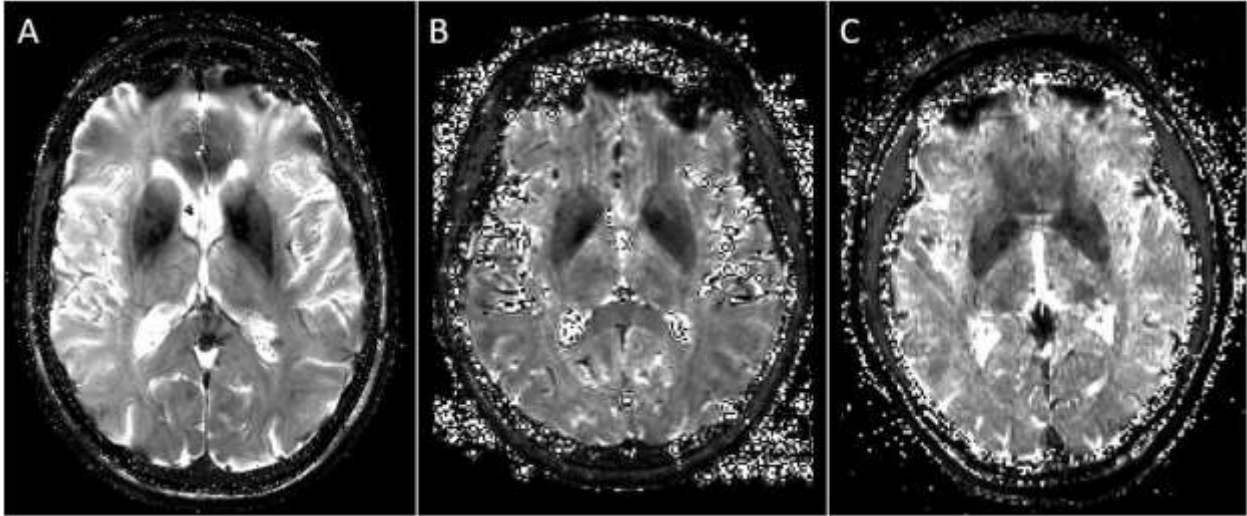


Figure 4.1 Axial views of the T2\* maps showing the globus pallidus. Due to slight differences in the imaging protocol, statistical comparisons were not performed across studies. A) ET study. B) PD study 1. C) PD study 2.

### Data Analysis

Manual regions of interest (ROIs) were drawn to segment the SN and GP in each subject to give an average T2\* value for each region (right and left were kept separate). ROIs were drawn in the axial plane by the same author (K.O.) in each study.

Statistical analysis was performed separately for each of the three studies in R (R Core Team, 2017). Group differences were tested using a linear regression with age and sex as covariates. Additionally, a linear regression of T2\* value and age was performed separately for each study to investigate a correlation between age and increased iron deposition.

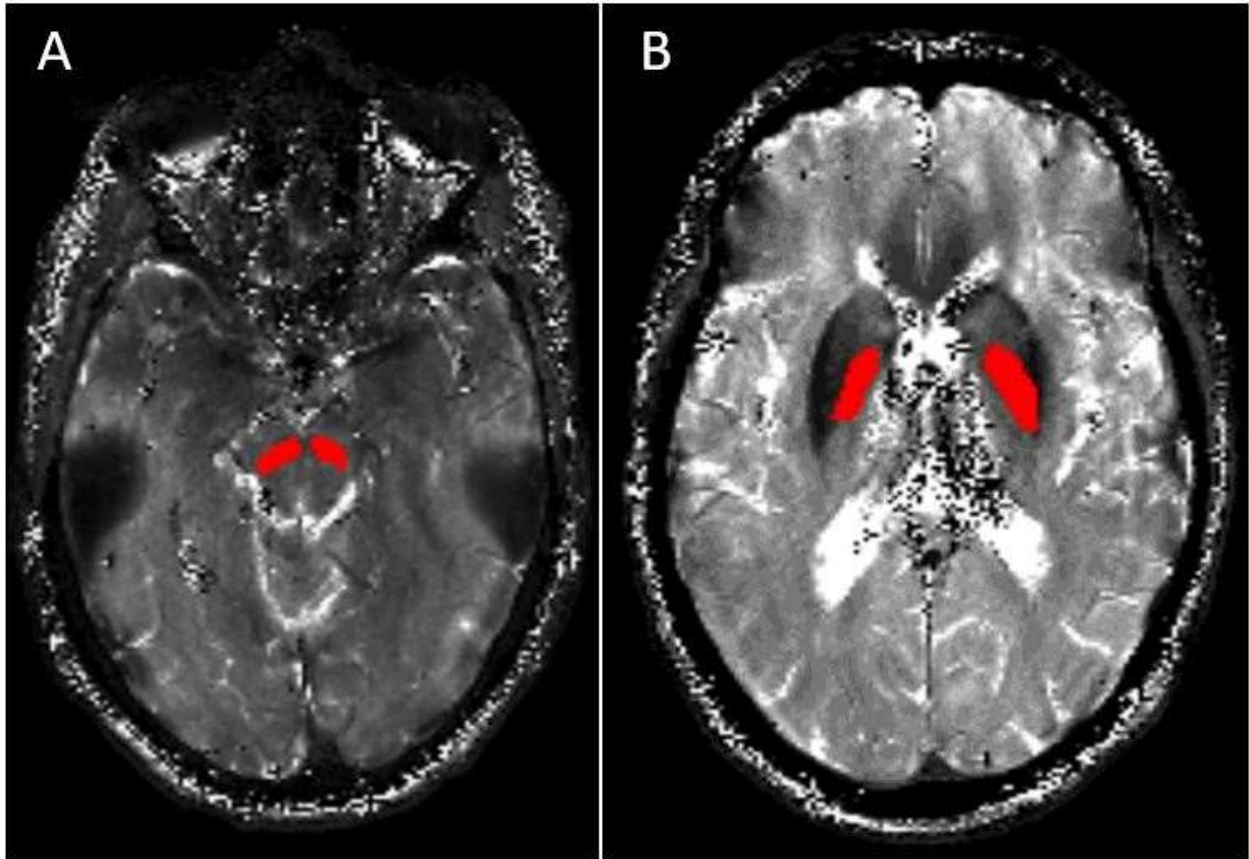


Figure 4.2 Axial views of the T2\* maps showing examples of the region of interest (ROI) placements in the A) substantia nigra (SN) and B) globus pallidus (GP). This example placement is performed on a control subject from the essential tremor study.

### 4.3 Results

There was no significant difference in age or sex between cases and controls in the ET study nor either of the PD studies. As previously mentioned, age and sex were factored into the regression for all groups, in part, to account for the documented increase in brain iron with aging in healthy subjects (Acosta-Cabronero et al., 2016; Ward et al., 2014).

PD cases had decreased T2\* in the right SN ( $p = 0.003$ ) compared to controls in PD study 1, indicating elevated iron deposition in this regions. Similarly, PD cases had decreased T2\* in the right SN ( $p = 0.039$ ) compared to controls in PD study 2, also indicating elevated iron deposition. Both PD study cases showed a similar pattern of decreased T2\* in the left SN, but the

differences were not significant. Neither PD study 1 or 2 showed a significant group difference in T2\* values in the GP. In the ET study, there was no significant group difference in T2\* value between cases and controls in the SN or the GP, indicating that there is no significant difference in iron deposition in ET. Additionally, there was no significant correlation between T2\* value and age in the SN or the GP in any of the three studies.

Table 4.1 Demographics presented by study and respective group. Mean and standard deviation of the region of interest analysis of T2\* in each group is presented by study, with linear regression p-values listed below each region by group. Note: Age and sex were used as nuisance variables in the linear regression.

Group	Age (mean±SD)	Sex	T2* (R_SN) (mean±SD)	T2* (L_SN) (mean±SD)	T2* (R_GP) (mean±SD)	T2* (L_GP) (mean±SD)
<b>ET Study</b>						
ET	78.1±6.6	11M/10F	12.35±4.27	12.63±4.36	12.96±4.01	12.46±3.87
ET Control	77.7±5.5	6M/6F	11.98±4.27	12.32±4.97	14.37±5.62	14.12±6.39
Linear regression p-value			0.695	0.766	0.431	0.356
<b>PD Study 1</b>						
PD1	60.1±6.2	5M/5F	23.11±2.87	25.17±2.72	24.45±3.19	24.31±2.67
PD1 Control	64.7±7.8	5M/2F	28.18±2.92	29.21±5.15	24.55±3.64	25.20±3.91
Linear regression p-value			<b>0.003</b>	0.072	0.883	0.481
<b>PD Study 2</b>						
PD 2	63.4±8.8	11M/10F	22.36±6.17	23.36±5.47	22.57±3.78	22.73±3.47
PD2 Control	58.9±10.3	11M/6F	27.04±6.21	27.02±6.00	24.13±4.93	25.43±4.47
Linear regression p-value			<b>0.039</b>	0.053	0.430	0.077

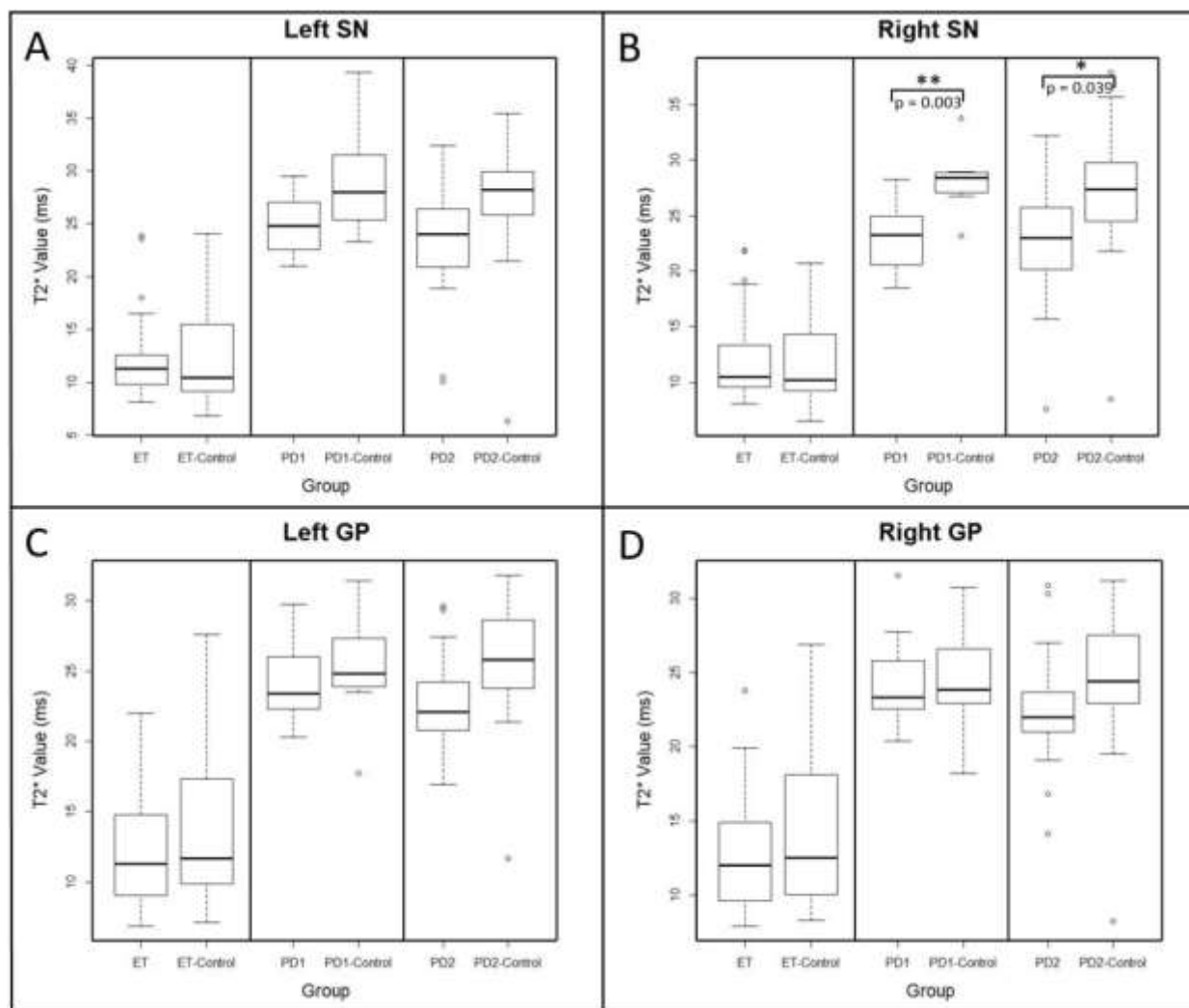


Figure 4.3 T2\* values for each region plotted by group for each study for A) Left SN, B) Right SN, C) Left GP, D) Right GP. Although plotted on the same scale, no direct comparison was performed between studies. Significant group differences were found in the Right SN in PD1 and PD2. Abbreviations: substantia nigra (SN), globus pallidus (GP), essential tremor (ET), Parkinson's disease study 1 (PD1), Parkinson's disease study 2 (PD2).

#### 4.4 Discussion

We investigated brain iron deposition in ET and PD using T2\* MRI, specifically in the SN and GP. Many prior studies have reported iron deposition in PD in the SN (Castellani et al., 2000; D. T. Dexter et al., 1987; D. T. T. Dexter et al., 1991; He et al., 2015; Homayoon et al., 2018; Langkammer et al., 2016; Ulla et al., 2013; Ward et al., 2014; Zecca et al., 2004), but few studies have been performed in ET (Homayoon et al., 2018; Novellino et al., 2013). Furthermore, there are inconsistent findings in the two published reports on iron deposition in ET. While both studies used R2\* ( $R2^* = 1/T2^*$ ) maps for quantification and had almost identical numbers of cases and controls, Novellino et al. (2013) used a whole brain, voxel-wise approach for identifying regions of increased iron. They reported an increase in iron in the bilateral SN, GP, and the right dentate nucleus, although only the GP remained significant after multiple comparison correction. Unfortunately, Novellino et al. (2013) does not report the mean R2\* values in the GP for each group, to demonstrate the extent of the difference.

Homayoon et al. (2018) used a manual segmentation approach, similar to the method presented in our study. They reported significantly increased iron in the SN in PD compared to Tremor in Dystonia, ET, and controls, but no significant difference between ET and any of the other three groups. Further, no significant difference between any of the four groups was found in the GP. Our study reproduces, in part, the results presented in Homayoon et al. (2018), with a significant increase in iron in the SN shown in PD cases compared to controls in two separate studies. Additionally, no significant change in iron in the SN or GP is shown in ET cases compared to controls. Although this is in contrast with the results of Novellino et al. (2013), it is in line with those presented by Homayoon et al. (2018).

This study attempted a whole brain, voxel-wise approach, but found that it was unreliable for multiple reasons. First, the quality of the data after resampling the T2\* maps to the resolution

of the 3D T1 weighted images was quite poor, especially in the ET study, due to the large slice thickness. Second, the registration of the brain stem and cerebellum is not as accurate as the cerebrum, and is often slightly out of alignment, even when registering the high-resolution T1-weighted images to the atlas. Therefore, results in the cerebellum and brainstem, where the SN resides, should be carefully investigated. Because of these difficulties, we opted for a less technical approach that avoids artifacts and is not reliant on image registration to investigate our two regions of interest.

This study is unique in that we are comparing the results from three separate studies using identical data processing and analysis, with the aim to show there is a reproducible increase in iron in the SN of PD cases as well as present a lack of increased brain iron in the SN and GP in ET cases. Specifically, we investigated the two PD cohorts as a validation of the sensitivity of our ROI method to detect group differences in T2\* signal irrespective of mild changes in imaging parameters. Additionally, we are able to show that the decrease in T2\* (which represents an increase in local iron) seen in the SN is consistent with previously published studies in PD. With the method validated by the two PD studies, we can more confidently present the lack of difference in T2\* signal in any region in ET compared to their control group.

Interestingly, we only find a significant decrease in T2\* in both PD groups in the right SN, not in the left. This is contrary to previously published results in PD, but figure 4.3 shows that there is still a visible decrease in T2\* in both PD groups in the left SN, the difference is just not significant. We believe this is likely due to small sample size and the large variance of the data, which is a result of the imaging protocol as well as the natural variation of iron abundance in the brain. Specifically in the ET study, the large slice thickness will contribute to the variance

due to partial volume effects and on individual slice positioning in each subject. This large variance could also be masking a potential group difference between ET cases and controls. Further investigation with high resolution (more isotropic resolution) data is needed to investigate this potential difference.

No correlation between T2\* value and age was found in either region for any of the three studies, although it has been shown that iron deposition does increase with age in healthy controls in the SN and GP (Acosta-Cabronero et al., 2016; Ward et al., 2014; Zecca et al., 2004). Importantly, the age span of observable change in brain iron reported in these studies is over the full adult lifespan (20 to 80 years of age). In fact, it is clear when looking at their data distributions that there is only an effect across the full range of ages. The age of subjects used in our three studies is not nearly this widespread (see table 4.1 for specific study age distributions), at most ranging from 44 to 82 (in PD study 2). Due to this relatively small distribution of ages (when compared to the full lifespan data) in these studies, together with the small sample size, it is not surprising not to find an overall effect of age on iron deposition in the SN.

This study has a few limitations; first, due to slight differences in MRI parameters, we chose not to directly compare the data from the different studies with one another. However, the results of the two PD studies, which reproduce previously reported findings, serves to validate the ability of the ROI method to detect a group difference in T2\* maps. Second, this study only investigated the SN and GP, and was unable to confidently implement the use of a voxel-wise analysis. With a consistent imaging sequence, and perhaps more isotropic resolution, a voxel-wise approach may be more viable and worth further investigation in these populations. Finally, due to the resolution of our images, we were unable to individually segment the two regions of the SN (pars compacta and pars reticulata), rather segmenting the SN as a whole.

#### **4.5 Conclusion**

This study investigated brain iron deposition in ET and PD with T2\* MRI in the SN and GP. Our results of increased iron deposition in the SN in PD was consistent across the two studies, providing evidence that the slight differences in imaging parameters of these two studies did not have a significant effect on the ability to detect group differences. However, the large slice thickness used in the ET study may have obscured a significant finding between cases and controls. Furthermore, the PD studies served to validate the ROI method, enabling more confident presentation of the lack of a significant increase in iron deposition in ET in either brain region. Due to the lack of consistent results across studies in ET, further investigation into iron deposition, using higher resolution and more accurate whole brain methods is warranted.

## 5. CONCLUSIONS AND FUTURE WORK

Essential Tremor is a commonly diagnosed disease which has been widely and actively studied, especially with the advent of non-invasive imaging methods. There is still much debate over the neurodegenerative hypothesis in ET as well as the best method to differentiate ET from other similar movement disorders. This thesis provides evidence for the neurodegenerative hypothesis, with support of gray matter density loss in the cerebellum and special attention having been paid to optimizing the methods for detecting gray matter volume loss in the cerebrum. Additionally, this thesis provides evidence of differences in T2\* iron quantification between ET and PD.

### 5.1 Neurodegeneration

The neurodegenerative hypothesis in ET is still actively debated, but this work provides strong evidence in support of this hypothesis. Chapters 2 and 3 not only add to the current pool of literature concerning gray matter volume loss in ET, but they also address an issue plaguing the existing literature: inconsistent and under-optimized methods. With the addition of higher resolution tissue probability maps and atlas, and the use of less constrained algorithms, our patterns of gray matter volume loss in ET, in both the cerebellum and cerebrum, were shown to be internally consistent between subgroups and biologically plausible.

Unfortunately, there is no gold standard method of physically verifying the accuracy of such brain segmentation processes. None the less, we must rely on consistency of results from group to group and from study to study, as well as logical end points to validate these methods. Our patterns of gray matter volume loss were consistent within subgroups, and shared multiple regions with reports from previous studies. Additionally, the patterns of gray matter volume loss

were consistent with identified motor paths in the brain, lending a logical plausibility to the result. Finally, no detection of gray matter volume *increase* was identified, which if present, would signify a methodological error, as this is not a valid biological result. Therefore, this thesis provides strong evidence to add to the current literature which supports the neurodegenerative hypothesis of ET.

## 5.2 Disease Differentiation

Ultimately, the value of research in disease is to better the identification and treatment of disease in the clinic. With such similar and often overlapping symptoms, the differentiation of ET and PD is an important matter of investigation. With non-invasive imaging studies working to improve our understanding of disease pathophysiology in-vivo, the potential for more concise diagnoses becomes more feasible. While disease differentiation is not always definitive, in-vivo imaging can provide additional diagnostic information that may allow for a more confident diagnosis.

Specifically with T2\* iron quantification, this thesis was able to demonstrate differences between ET and PD cases on a group level. Iron deposition in the brain is a quantifiable difference between ET and PD, with this thesis providing evidence for a lack of increased iron accumulation in the brain in ET (as seen in PD). However, the extent of iron deposition throughout the whole brain needs further investigation, especially in ET to make this a viable tool for disease distinction. Furthermore, additional analysis is needed to prove the ability to detect an increase in regional brain iron on an individual basis.

### 5.3 Future Works

As previously mentioned, further investigation into iron deposition in the brains of ET cases is warranted for this method to aid in the diagnosis of ET and PD. Specifically, an accurate whole-brain approach needs to be developed to establish if an ET case-control group difference exists anywhere in the brain, not just in two regions of interest in the disease. To further improve this whole-brain approach, Quantitative Susceptibility Mapping in addition to T2\* mapping should be considered for iron quantification, as this has been suggested to be a more robust approach at quantifying the magnetic field effect of local iron in the brain. In addition, inclusion of PD cases with this proposed study would serve to validate the updated methods against previously published literature on brain iron in PD, while also investigating a potential group difference between ET and PD cases as well. Finally, receiver operating characteristic (ROC) analysis could be performed to initially test the diagnostic viability of iron quantification imaging. Furthermore, machine learning could be applied to determine if disease state can be predicted by region brain iron accumulation, perhaps in conjunction with other established disease biomarkers.

## APPENDIX

### **Essential Tremor vs. Parkinson Disease: Neurometabolite Differences Using GABA-Edited Spectroscopy**

#### **Introduction**

Essential tremor (ET), one of the most common movement disorders, is characterized by kinetic tremor of the upper extremities. Additionally, tremor may be present in cranial structures such as the neck, voice or jaw (Benito-León & Labiano-Fontcuberta, 2016). Clinically, the differentiation of ET from Parkinson's disease (PD) may be challenging, as cases may present with overlapping clinical features; indeed, studies have shown that a high number of supposed ET cases have PD (Jain, Lo, & Louis, 2006). It has also been shown that there is significant elevation of GABA in the basal ganglia of PD cases, and there is active investigation of the correlation between GABA and PD subtypes (Emir, Tuite, & Öz, 2012; O'Gorman Tuura, Baumann, & Baumann-Vogel, 2018). With ET and PD sharing similar symptoms as well as disease pathology, investigation of GABA in ET is warranted. Specifically, comparing thalamic GABA in ET and PD could provide evidence of whether elevated GABA is a unique feature of PD, or rather a general feature in diseases with tremor.

The thalamus likely plays some role in the pathophysiology of both ET and PD, due to its many connections to various motor circuits throughout the brain and its putative role in tremor circuitry. Indeed, the cerebello-thalamo-cortical loop, comprising highly organized connections between the cerebellum, deep brain structures including the thalamus, and the motor cortex, has been posited to be involved in the origins and propagation of tremor in both ET and PD (Helmich, Toni, Deuschl, & Bloem, 2013; Lenka et al., 2017; Muthuraman et al., 2018; Oz,

2016, Chapter 7). Few studies, though, have investigated alterations in neurometabolites in the thalamus of these disease groups.

Input to the motor thalamus is both gamma-aminobutyric acid (GABA)-ergic (from the basal ganglia) and glutamatergic (from the deep cerebellar nuclei); output from the motor thalamus to the motor cortex is glutamatergic, making these transmitters of prime interest in magnetic resonance spectroscopy (MRS) studies of this brain structure.

In ET, one study using short echo time MRS reported an increase in thalamic Glx compared to controls (Barbagallo et al., 2018). The study had a reasonable sample size (16 ET cases vs 14 controls) but was unable to report data on thalamic GABA due to the choice of the MRS sequence, as a special spectral editing sequence is necessary for accurate quantification of GABA. In PD, one study reported lower Glx and higher GABA in the thalamus of akinetic PD cases (Pesch et al., 2019). The study had a reasonable sample size (19 akinetic PD cases vs 35 controls) and used a J-editing sequence similar to those presented in our study for metabolite quantification. However, the study does not find a significant difference in any metabolites between the combined PD group (35 cases) and controls (Pesch et al., 2019). Additionally, another previous study has reported elevated GABA in the basal ganglia of PD cases compared to controls using similar spectral editing methods (O’Gorman Tuura et al., 2018).

The current study aims to investigate differences in thalamic GABA between ET cases and controls and to compare them to the results of increased thalamic Glx in ET cases and elevated thalamic GABA in PD cases using GABA edited MRS.

## **Methods**

### **ET Subjects**

Subjects in this study are a subset of a larger study on GABA levels in ET in the cerebellum (Louis et al., 2018). ET cases were recruited (2013-2016) from a clinical-

epidemiological study of ET, the neurological practice of one of the authors (E.D.L), and via study advertisements. Inclusion criteria included a priori diagnosis of ET assigned by the treating neurologist and willingness to undergo MRI. Exclusion criteria included heavy ethanol exposure (Harasymiw & Bean, 2001), history of a neurodegenerative disease (PD, Alzheimer's disease), prior deep brain stimulation or other neurosurgery, or contraindication for MRI. Additionally, we excluded cases who were taking medications that bind to the GABA<sub>A</sub> receptor or that enhance GABA tone (e.g., clonazepam, diazepam, lorazepam, gabapentin, phenobarbital, progabide, propofol, tiagabine, valproate, vigabatrin). 24 ET cases were recruited for this study, but 3 cases were excluded from analysis due to fitting errors of the metabolite concentration greater than 20% (25% for GABA). Therefore, 21 ET cases are presented in this study (age  $77.6 \pm 5.7$  yrs).

5 control subjects (age  $79.6 \pm 6.7$  yrs) were recruited during the same time period and from the same sources as the ET cases, with some being the spouses of ET cases. Exclusion criteria included a history of ET or a family history of ET (first- or second-degree relative) or presence on two hand-drawn screening Archimedes spirals of a tremor rating  $>1$  (rated by a senior neurologist specializing in movement disorders (E.D.L.) who used the Washington Heights-Inwood Genetic Study of ET (WHIGET) tremor rating scale) (Louis, 2015; Louis et al., 2018).

A videotaped neurological examination was performed on all ET cases and controls, and was rated using the WHIGET tremor rating scale, to rate postural and kinetic tremor during each test of a set of 12 tests: 0 (none), 1 (mild), 2 (moderate), and 3 (severe). Diagnosis of ET was reconfirmed by E.D.L. using the videotaped neurological examination and WHIGET diagnostic criteria (moderate or greater amplitude kinetic tremor [tremor rating  $\geq 2$ ] during at least three

tests or a head tremor, in the absence of Parkinson's disease, dystonia, or another cause) (Louis et al., 2018).

Images for the ET study were acquired on a Siemens 3T Prisma (Siemens Healthcare, Erlangen, Germany). Image acquisition included a 3D T1 weighted MPRAGE (TR/TE/TI = 2300/ 2.94/ 900 ms, flip angle = 9°, 1.0x1.0x1.2 mm<sup>3</sup>) for determination of tissue fractions of the MRS volume of interest (VOI). The MEGA-PRESS J-editing sequence was used for GABA detection (TR/TE = 1500/68 ms, 25x25x25 mm<sup>3</sup>, 196 averages) (Mullins et al., 2014). One series is acquired with the spectrally selective editing pulse centered at 1.9 ppm (edit-on), and another series with the editing pulse centered at 7.5 ppm (edit-off) in an interleaved fashion. The difference spectrum from these two scans was used for quantification of GABA. A single MEGA-PRESS VOI was placed in the right thalamus for each subject (Figure 1A). The PRESS short echo time MRS sequence (TR/TE = 1500/30 ms, 25x25x25 mm<sup>3</sup>, 128 averages) used the same VOI placement as the MEGA-PRESS sequence. Creatine (Cr), N-Acetyl Aspartate (NAA), Glu, Glx, Choline (Cho), and myo-Inositol (mI) were quantified from the PRESS sequence.

This study was approved by the Yale University, Purdue University, and Weill Cornell Medical College Institutional Review Board. Written informed consent was obtained from each subject upon enrollment in the study.

### **PD Subjects**

Subjects for the PD part of this study had been recruited for a previous study on GABA levels in various brain regions in PD (Dharmadhikari et al., 2015). PD cases (recruited in 2014) were assessed using the motor part of the Unified Parkinson's Disease Rating Scale (UPDRS-III) by a trained neurologist (S.E.Z). The grooved pegboard test (Lafayette Instrument, Lafayette, Indiana, USA), was used to assess the motor performance in all subjects (Merker & Podell,

2011). Three PD cases were medication naïve, while the remaining cases did not take any Parkinson's medication for at least 12 hours prior to the study. Exclusion criteria included any previous history of neurological disorders, dementia, severe rest tremor, current daily use of GABA-ergic drugs (e.g. gabapentin, benzodiazapines), or contraindication for MRI.

Images for the PD study were acquired on a Siemens 3T Trio (Siemens Healthcare, Erlangen, Germany) on 18 PD cases, and 17 Controls. One PD cases and one control were excluded from statistical analysis due to fitting errors of the metabolite concentration greater than 20% (25% for GABA), thus this study reports on 17 PD cases (age  $63.2 \pm 9.2$  yrs) and 16 controls (age  $59.1 \pm 10.3$  yrs) from the previous PD study group. The images acquired included a 3D T1 weighted MPRAGE (TR/TE/TI = 2300/ 2.94/ 900 ms, flip angle =  $9^\circ$ ,  $1.0 \times 1.0 \times 1.2$  mm<sup>3</sup>). The MEGA-PRESS J-editing sequence was used for GABA detection (TR/TE = 2000/68 ms,  $25 \times 30 \times 25$  mm<sup>3</sup>, 128 averages) (Mescher, Merkle, Kirsch, Garwood, & Gruetter, 1998; Mullins et al., 2014). One series was acquired with the spectrally selective editing pulse centered at 1.9 ppm (edit-on), and another series was acquired with the editing pulse centered at 7.5 ppm (edit-off) in an interleaved fashion. The difference spectrum from these two scans was used for quantification of GABA. A single MEGA-PRESS VOI was placed in the right thalamus for each subject (Figure 1B). The PRESS short echo time MRS sequence (TR/TE = 2000/35 ms,  $25 \times 30 \times 25$  mm<sup>3</sup>, 32 averages) used the same VOI placement as the MEGA-PRESS sequence. Cr, NAA, Glu, Glx, Cho, and mI were quantified from the PRESS sequence.

This study was approved by the Indiana University Institutional Review Board. Written informed consent was obtained from each subject upon enrollment in the study

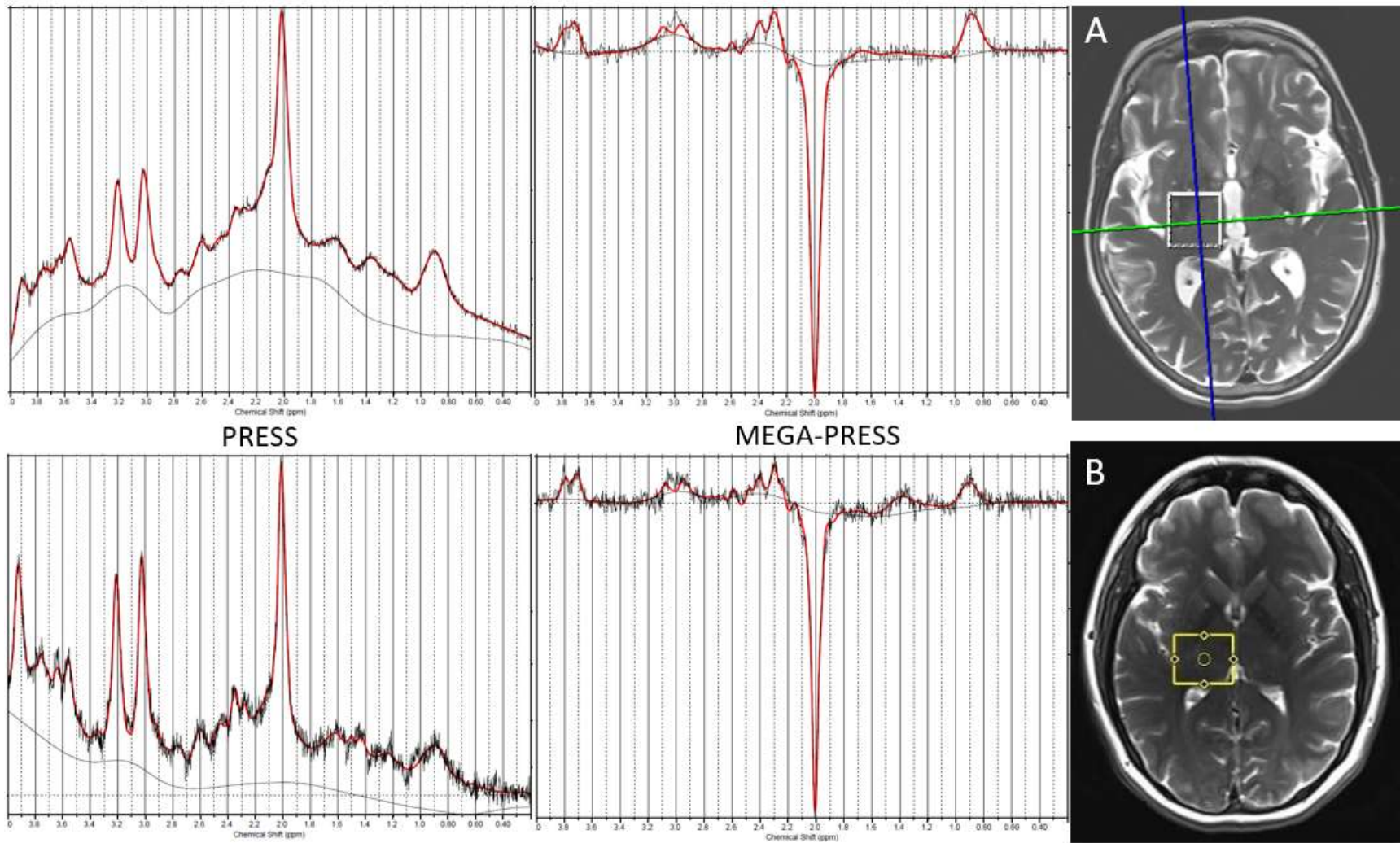


Figure 1 PRESS, MEGA-PRESS edited spectra, and VOI placement on axial T2 image. A) ET study spectrum (PRESS left, MEGA-PRESS right) and placement. B) PD study spectrum (PRESS left, MEGA-PRESS right) and placement.

## Spectral Processing

Quantification of MEGA-PRESS and PRESS spectra was performed in LCModel (v 6.2-0R) which applies a linear combination of basis sets to fit the spectra (Provencher, 1993). These basis sets were generated from density matrix simulations of the sequence and published values of chemical shifts and coupling constants (Kaiser, Young, Meyerhoff, Mueller, & Matson, 2008). Tissue segmentation of the 3D T1 weighted image was performed in SPM12 and voxel co-registration was performed using an in-house tool built in MATLAB (v R2018a). This tool corrects the output from LCModel by multiplying by a water correction factor from LCModel (FCALIB factor) and calculates a CSF corrected value for each metabolite (Chowdhury et al., 2015).

Ideally, this study had proposed to look only at metabolic differences between ET cases and controls. Due to the lack of thalamic data in controls from the ET study, we proposed instead to compare the ET study data with the PD study data (specifically for the control population data). Unfortunately, this came with an added complication of different age populations (mean age of ET study subjects ~ 78, mean age of PD study subjects ~ 61) as well as notable differences in MRS sequences, especially the PRESS sequence. Comparing metabolites quantified from the edited OFF spectra would have been preferred to comparing the different PRESS sequences, as only the TR and voxel size differ. However, due to poor signal to noise ratio (SNR), this data could not be used. Therefore, an attempt at correcting the PRESS data to make the sequences comparable was performed.

To attempt to account for the differences in imaging sequence, these same sequences were performed on one healthy consenting volunteer during the same scan session. Using the data from this test, empirical correction factors were calculated for each differing factor (TR, TE, number of averages, and voxel size/placement). Additionally, theoretical correction factors were

calculated to assess the accuracy of our empirical correction factors. To correct for TR, we calculated the ratio of the signals using the Bloch equation, using empirical T1 values for each metabolite from the literature (Puts, Barker, & Edden, 2013; Träber, Block, Lamerichs, Gieseke, & Schild, 2004). TE correction could not be theoretically calculated, due to a change in MRI scanner pulse shape between TEs of 30 and 35 ms. The number of averages scales with the square root, and the voxel size is a linear correction. Finally, a direct empirical factor was calculated as the ratio of the PD sequence divided by the ET sequence for each metabolite. ET-corrected PRESS data was then the product of the LCModel result and this empirical correction factor.

### **Statistical Analysis**

Analysis of Variance (ANOVA) with a Tukey HSD post-hoc test was performed to determine significant group differences between each of the four groups; ET, ET-Control, PD, and PD-Control. Age and sex were used as covariates in the analysis.

Table 1. Subject demographics, metabolite concentration means (approx. in mM) and standard deviations by study group. P-values for ANOVA and Tukey HSD tests presented by group for each metabolite

	Age (Mean±St Dev)	Sex	Cr	GABA	Glu	Glx	NAA	Cho	mI
ET Cases	77.6±5.7	12M/12F	5.0±0.6	2.3±0.6	4.7±1.0	6.8±1.7	8.0±0.6	1.6±0.3	2.6±0.5
ET Controls	79.6±6.7	1M/4F	4.6±0.3	2.2±0.3	4.4±0.7	6.2±1.3	7.9±0.3	1.4±0.2	2.4±0.2
PD Cases	63.2±9.2	9M/8F	5.4±0.6	2.5±0.4	5.1±0.7	10.8±1.6	7.4±0.8	1.7±0.1	1.8±0.2
PD Controls	59.1±10.3	9M/7F	5.6±0.6	2.1±0.4	5.6±0.9	11.9±1.8	7.6±0.8	1.7±0.1	2.0±0.4
ANOVA	<b>&lt;0.001</b>	-	<b>0.003</b>	0.224	<b>0.010</b>	<b>&lt;0.001</b>	0.0584	<b>0.037</b>	<b>&lt;0.001</b>
ET vs ET-C	0.962	-	0.568	-	0.916	0.8825	-	0.366	0.640
ET vs PD	<b>&lt;0.001</b>	-	0.237	-	0.349	<b>&lt;0.001</b>	-	0.726	<b>&lt;0.001</b>
ET vs PD-C	<b>&lt;0.001</b>	-	<b>0.014</b>	-	<b>0.015</b>	<b>&lt;0.001</b>	-	0.233	<b>&lt;0.001</b>
PD vs ET-C	<b>0.002</b>	-	0.081	-	0.351	<b>&lt;0.001</b>	-	0.127	0.072
ET-C vs PD-C	<b>&lt;0.001</b>	-	<b>0.011</b>	-	0.059	<b>&lt;0.001</b>	-	<b>0.036</b>	0.268
PD vs PD-C	0.503	-	0.644	-	0.528	0.249	-	0.841	0.785

## Results

There exists a significant difference in age between groups (ANOVA  $p < 0.001$ ), specifically between ET vs PD ( $p < 0.001$ ), ET vs PD-C ( $p < 0.001$ ), PD vs ET-C ( $p = 0.002$ ), and ET-C vs PD-C ( $p < 0.001$ ). This indicates that there is a significant difference in age between the two study populations. Age and sex were used as covariates in all following statistical tests. Post hoc (Tukey HSD) tests were only performed on metabolites with a significant ANOVA.

The ANOVA was significant for Cr ( $p = 0.003$ ), Glu ( $p = 0.010$ ), Glx ( $p < 0.001$ ), Cho ( $p = 0.037$ ), and mI ( $p < 0.001$ ). Cr was significantly decreased in ET vs PD-C ( $p = 0.014$ ) and ET-C vs PD-C ( $p = 0.011$ ). Glu was significantly decreased in ET vs PD-C ( $p = 0.015$ ). Glx was significantly decreased in ET vs PD, ET vs PD-C, ET-C vs PD, and ET-C vs PD-C (all  $p < 0.001$ ). This is indicative of a systematic bias between the two study methods. Cho was significantly decreased in ET-C vs PD-C ( $p = 0.036$ ). mI was significantly increased in ET vs PD and ET vs PD-C (both  $p < 0.001$ ). Additionally, when only PD and PD-C were compared with a linear regression, GABA was significantly elevated in PD ( $p = 0.025$ ).

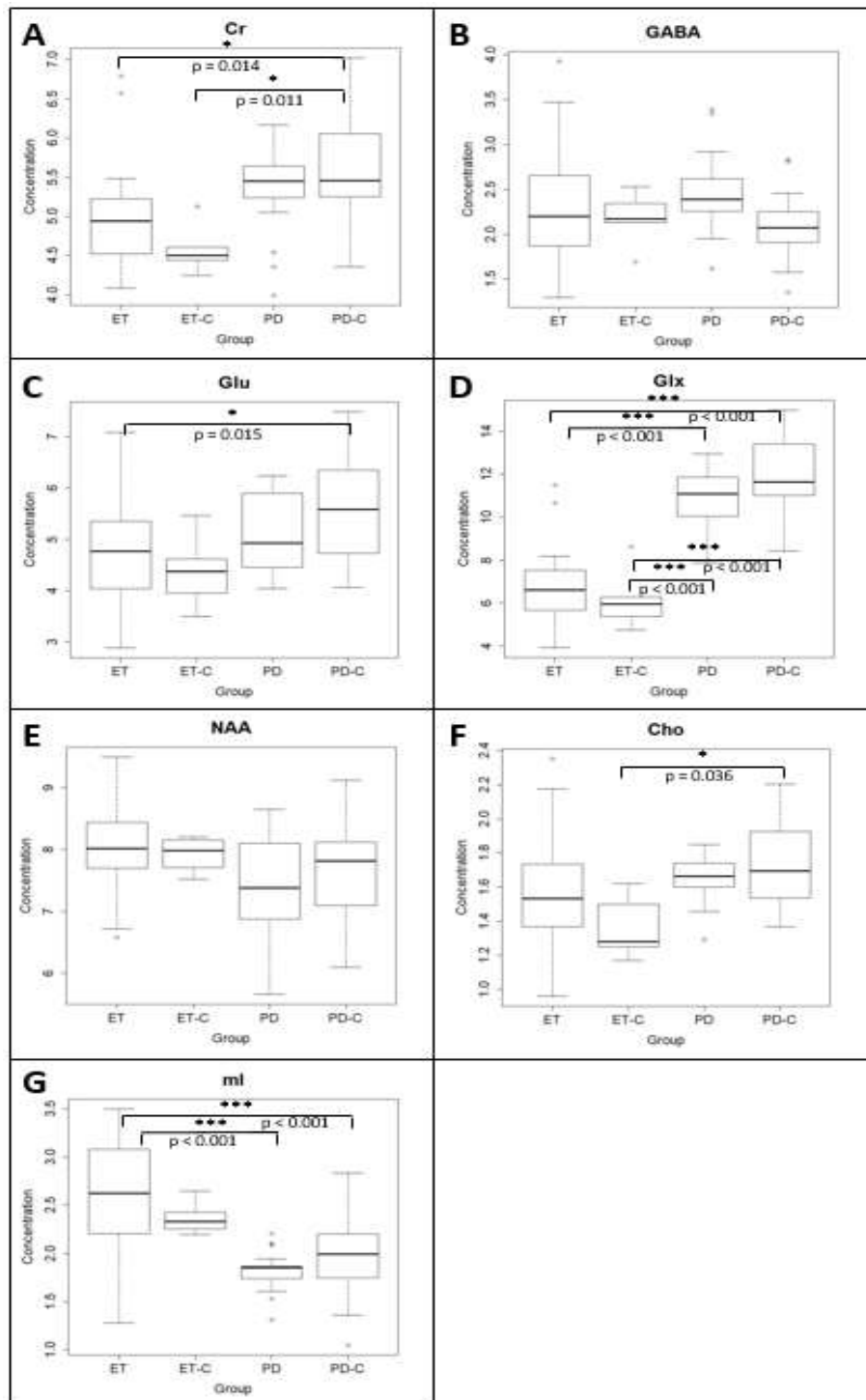


Figure 2 Boxplots showing median and upper and lower quartiles of thalamic metabolites for ET, ET-Controls (ET-C), PD, and PD-Controls (PD-C). A) Cr B) GABA. C) Glu D) Glx E) NAA F) Cho G) ml

## Discussion

To our knowledge, this is the first study investigating metabolic changes in ET with GABA-edited MRS in the thalamus. One previous study has reported increased thalamic Glx/Cr in ET (Barbagallo et al., 2018) using PRESS short echo time MRS. Our study, however, uses MEGA-PRESS for a more accurate quantification of GABA. Unfortunately, while our study has a similar number of cases compared to the previous study, the number of ET controls was too low to allow proper statistical comparisons. In an attempt to account for this low number of control subjects, we compared the ET study with the PD study. In the PD literature, one previous study presented an increase in thalamic GABA in akinetic-PD (Pesch et al., 2019). Our study also presents a significant increase in thalamic GABA in PD compared to controls. This result is consistent with other literature presenting increased GABA in the basal ganglia of PD cases as well ((Emir et al., 2012; O’Gorman Tuura et al., 2018).

It is important to note that there are no significant differences between case and controls groups *within* our studies (neither ET nor PD study) for any metabolites assessed by PRESS. Additionally, there are multiple factors that serve to invalidate the statistically significant differences that are reported. First and foremost, the image acquisition for the two studies was considerably different. The PRESS sequences differed on many parameters (TR, TE, averages, and voxel size/placement) and the MEGA-PRESS sequences had different TRs, averages, and voxel size/placement. As previously described, empirical correction factors were derived in an attempt to account for these differences. Many of the empirical correction factors were even within measurement error (except for TR correction) of theoretical corrections.

The two studies also differed significantly with respect to age, with the ET study population being significantly older than the PD population. Unfortunately, we could only

include age as a covariate in an attempt to account for the difference between studies, but this does not entirely eliminate the affect.

These corrections seem to have been ineffective in allowing comparability between these two studies however, as the significant differences in Cr and Cho between the studies are indicative of a systematic error (namely, the different sequence). An age difference between the studies would not explain these differences either. Therefore, we believe we were unsuccessful in correcting the data for comparability between studies. Although we report significant differences, we believe this data is inconclusive due to the reasons discussed above. Further investigation is warranted with identical imaging parameters and better age matched participants.

### **Conclusion**

Although this study presents statistically significant differences in multiple metabolites, due to the differences in imaging parameters and population age, this data is inconclusive regarding metabolic group differences in the thalamus. Investigation of metabolic differences in the thalamus between ET and PD is still of great interest, with potentially clinical value. Future studies require identical and optimized imaging protocols and an age matched population across both disease groups and controls.

## REFERENCES

- Acosta-Cabronero, J., Betts, M. J., Cardenas-Blanco, A., Yang, S., & Nestor, P. J. (2016). In Vivo MRI Mapping of Brain Iron Deposition across the Adult Lifespan. *Journal of Neuroscience*, *36*(2), 364–374. <http://doi.org/10.1523/JNEUROSCI.1907-15.2016>
- Aschner, M., Erikson, K. M., Hernández, E., & Tjalkens, R. (2009). Manganese and its Role in Parkinson's Disease: From Transport to Neuropathology, *73*(4), 389–400. <http://doi.org/10.1530/ERC-14-0411.Persistent>
- Ashburner, J. (2009). Computational anatomy with the SPM software. *Magnetic Resonance Imaging*, *27*(8), 1163–1174. <http://doi.org/10.1016/j.mri.2009.01.006>
- Ashburner, J. (2010). VBM Tutorial. Retrieved from [www.fil.ion.ucl.ac.uk/~john/misc/VBMclass10.pdf](http://www.fil.ion.ucl.ac.uk/~john/misc/VBMclass10.pdf)
- Ashburner, J., & Friston, K. J. (2000). Voxel-Based Morphometry—The Methods. *NeuroImage*, *11*(6), 805–821. <http://doi.org/10.1006/nimg.2000.0582>
- Ashburner, J., & Friston, K. J. (2005). Unified segmentation. *NeuroImage*, *26*(3), 839–851. <http://doi.org/10.1016/j.neuroimage.2005.02.018>
- Bagepally, B. S., Bhatt, M. D., Chandran, V., Saini, J., Bharath, R. D., Vasudev, M. K., ... Pal, P. K. (2012). Decrease in cerebral and cerebellar gray matter in essential tremor: A voxel-based morphometric analysis under 3T MRI. *Journal of Neuroimaging*, *22*(3), 275–278. <http://doi.org/10.1111/j.1552-6569.2011.00598.x>
- Barbagallo, G., Arabia, G., Novellino, F., Nisticò, R., Salsone, M., Morelli, M., ... Quattrone, A. (2018). Increased glutamate + glutamine levels in the thalamus of patients with essential tremor: A preliminary proton MR spectroscopic study. *Parkinsonism and Related Disorders*, *47*, 57–63. <http://doi.org/10.1016/j.parkreldis.2017.11.345>
- Benito-León, J. (2014). Essential tremor: a neurodegenerative disease? *Tremor Other Hyperkinet Mov (N Y)*, *4*, 252. <http://doi.org/10.7916/D8765CG0>
- Benito-León, J., Alvarez-Linera, J., Hernández-Tamames, J. A., Alonso-Navarro, H., Jiménez-Jiménez, F. J., & Louis, E. D. (2009). Brain structural changes in essential tremor: Voxel-based morphometry at 3-Tesla. *Journal of the Neurological Sciences*, *287*(1–2), 138–142. <http://doi.org/10.1016/j.jns.2009.08.037>
- Benito-León, J., & Labiano-Fontcuberta, A. (2016). Linking Essential Tremor to the Cerebellum: Clinical Evidence. *Cerebellum*, *15*(3), 253–262. <http://doi.org/10.1007/s12311-015-0741-1>
- Benjamini, Y., & Hochberg, Y. (1995). Controlling the False Discovery Rate : A Practical and Powerful Approach to Multiple Testing. *Journal of the Royal Statistical Society*, *57*(1), 289–300.

- Bhalsing, K. S., Upadhyay, N., Kumar, K. J., Saini, J., Yadav, R., Gupta, A. K., & Pal, P. K. (2014). Association between cortical volume loss and cognitive impairments in essential tremor. *European Journal of Neurology*, *21*(6), 874–883. <http://doi.org/10.1111/ene.12399>
- Blakemore, S. J., Chris, F. D., & Wolpert, D. M. (2001). The cerebellum is involved in predicting the sensory consequences of action. *Neuroreport*, *12*(9), 1879–1884.
- Broersma, M., Van Der Stouwe, A. M. M., Buijink, A. W. G., De Jong, B. M., Groot, P. F. C., Speelman, J. D., ... Maurits, N. M. (2016). Bilateral cerebellar activation in unilaterally challenged essential tremor. *NeuroImage: Clinical*, *11*, 1–9. <http://doi.org/10.1016/j.nicl.2015.12.011>
- Buijink, A. W. G., Broersma, M., van der Stouwe, A. M. M., Sharifi, S., Tijssen, M. A. J., Speelman, J. D., ... van Rootselaar, A. F. (2015). Cerebellar Atrophy in Cortical Myoclonic Tremor and Not in Hereditary Essential Tremor—a Voxel-Based Morphometry Study. *Cerebellum*. <http://doi.org/10.1007/s12311-015-0734-0>
- Cameron, E., Dyke, J. P., Hernandez, N., Louis, E. D., & Dydak, U. (2018). Cerebral gray matter volume losses in essential tremor: A case-control study using high resolution tissue probability maps. *Parkinsonism and Related Disorders*, *51*, 85–90. <http://doi.org/10.1016/j.parkreldis.2018.03.008>
- Castellani, R. J., Siedlak, S. L., Perry, G., & Smith, M. A. (2000). Sequestration of iron by Lewy bodies in Parkinson's disease. *Acta Neuropathologica*, *100*(2), 111–114. <http://doi.org/10.1007/s004010050001>
- Cauda, F., D'Agata, F., Sacco, K., Duca, S., Geminiani, G., & Vercelli, A. (2011). Functional connectivity of the insula in the resting brain. *NeuroImage*, *55*(1), 8–23. <http://doi.org/10.1016/j.neuroimage.2010.11.049>
- Cerasa, A., Messina, D., Nicoletti, G., Novellino, F., Lanza, P., Condino, F., ... Quattrone, A. (2009). Cerebellar atrophy in essential tremor using an automated segmentation method. *American Journal of Neuroradiology*, *30*(6), 1240–1243. <http://doi.org/10.3174/ajnr.A1544>
- Cerasa, A., & Quattrone, A. (2016). Linking Essential Tremor to the Cerebellum: Neuroimaging Evidence. *Cerebellum*, *15*(3), 263–275. <http://doi.org/10.1007/s12311-015-0739-8>
- Chavhan, G. B., Babyn, P. S., Thomas, B., Shroff, M. M., & Haacke, E. M. (2009). Principles, Techniques, and Applications of T2\*-based MR Imaging and Its Special Applications. *RadioGraphics*, *29*(5), 1433–1449. <http://doi.org/10.1148/rg.295095034>
- Chen, F.-X., Kang, D.-Z., Chen, F.-Y., Liu, Y., Wu, G., Li, X., ... Lin, Z.-Y. (2016). Gray matter atrophy associated with mild cognitive impairment in Parkinson's disease. *Neuroscience Letters*, *617*, 160–165. <http://doi.org/10.1016/j.neulet.2015.12.055>
- Choe, M., Cortés, E., Vonsattel, J. P. G., Kuo, S. H., Faust, P. L., & Louis, E. D. (2016). Purkinje cell loss in essential tremor: Random sampling quantification and nearest neighbor analysis. *Movement Disorders*, *31*(3), 393–401. <http://doi.org/10.1002/mds.26490>

- Choi, S.-M., Kim, B. C., Chang, J., Choi, K.-H., Nam, T.-S., Kim, J.-T., ... de Leon, M. J. (2015). Comparison of the Brain Volume in Essential Tremor and Parkinson's Disease Tremor Using an Automated Segmentation Method. *European Neurology*, *73*(5–6), 303–9. <http://doi.org/10.1159/000381708>
- Chowdhury, F. A., O’Gorman, R. L., Nashef, L., Elwes, R. D., Edden, R. A., Murdoch, J. B., ... Richardson, M. P. (2015). Investigation of glutamine and GABA levels in patients with idiopathic generalized epilepsy using MEGAPRESS. *Journal of Magnetic Resonance Imaging*, *41*(3), 694–699. <http://doi.org/10.1002/jmri.24611>
- Daniels, C., Peller, M., Wolff, S., Alfke, K., Witt, K., Gaser, C., ... Deuschl, G. (2006). Voxel-based morphometry shows no decreases in cerebellar gray matter volume in essential tremor. *Neurology*, *67*(8), 1452–1456. <http://doi.org/10.1212/01.wnl.0000240130.94408.99>
- Dexter, D. T. T., Carayon, A., Javoy-Agid, F., Agid, Y., Wells, F. R. R., Daniel, S. E. E., ... Marsden, C. D. D. (1991). Alterations in the Levels of Iron , Ferritin and Other Trace Metals in Parkinson ’ S Disease and Other Neurodegenerative. *Brain.*, *114*(Pt 4), 1953–1975. <http://doi.org/10.1093/brain/114.4.1953>
- Dexter, D. T., Wells, F. R., Agid, F., Agid, Y., Lees, A. J., Jenner, P., & Marsden, C. D. (1987). Increased Nigral Iron Content in Postmortem Parkinsonian Brain. *The Lancet*, *330*(8569), 1219–1220. [http://doi.org/10.1016/S0140-6736\(87\)91361-4](http://doi.org/10.1016/S0140-6736(87)91361-4)
- Dharmadhikari, S., Ma, R., Yeh, C. L., Stock, A. K., Snyder, S., Zauber, S. E., ... Beste, C. (2015). Striatal and thalamic GABA level concentrations play differential roles for the modulation of response selection processes by proprioceptive information. *NeuroImage*, *120*, 36–42. <http://doi.org/10.1016/j.neuroimage.2015.06.066>
- Diedrichsen, J. (2006). A spatially unbiased atlas template of the human cerebellum. *NeuroImage*, *33*(1), 127–138. <http://doi.org/10.1016/j.neuroimage.2006.05.056>
- Diedrichsen, J., Balsters, J. H., Flavell, J., Cussans, E., & Ramnani, N. (2009). A probabilistic MR atlas of the human cerebellum. *NeuroImage*, *46*(1), 39–46. <http://doi.org/10.1016/j.neuroimage.2009.01.045>
- Diedrichsen, J., & Zotow, E. (2015). Surface-based display of volume-averaged cerebellar imaging data. *PLoS ONE*, *10*(7), 1–18. <http://doi.org/10.1371/journal.pone.0133402>
- Dohlinger, S., Hauser, T.-K., Borkert, J., Luft, A. R., & Schulz, J. (2008). Magnetic Resonance Imaging in Spinocerebellar Ataxias. *The Cerebellum*, *7*(1), 204–214. <http://doi.org/10.1007/s12311-008-00>
- Dydak, U., Dharmadhikari, S., Snyder, S., & Zauber, S. E. (2015). Increased Thalamic GABA Levels Correlate with Parkinson Disease Severity. Nice, France: Neurodegenerative Diseases.

- Dyke, J. P., Cameron, E., Hernandez, N., Dydak, U., & Louis, E. D. (2017). Gray matter density loss in essential tremor : a lobule by lobule analysis of the cerebellum. *Cerebellum & Ataxias*, 4(1), 1–7. <http://doi.org/10.1186/s40673-017-0069-3>
- Emir, U. E., Tuite, P. J., & Öz, G. (2012). Elevated pontine and putamenal gaba levels in mild-moderate parkinson disease detected by 7 tesla proton mrs. *PLoS ONE*, 7(1). <http://doi.org/10.1371/journal.pone.0030918>
- Filip, P., Lungu, O. V, Manto, M., & Bares, M. (2016). Linking Essential Tremor to the Cerebellum : Physiological Evidence. *Cerebellum*, 15(6), 774–780. <http://doi.org/10.1007/s12311-015-0740-2>
- Fonov, V., Evans, A. C., Botteron, K., Almli, C. R., McKinstry, R. C., & Collins, D. L. (2011). Unbiased average age-appropriate atlases for pediatric studies. *NeuroImage*, 54(1), 313–327. <http://doi.org/10.1016/j.neuroimage.2010.07.033>
- Fonov, V., Evans, A., McKinstry, R., Almli, C., & Collins, D. (2009). Unbiased nonlinear average age-appropriate brain templates from birth to adulthood. *NeuroImage*, 47, S102. [http://doi.org/10.1016/S1053-8119\(09\)70884-5](http://doi.org/10.1016/S1053-8119(09)70884-5)
- Frisoni, G. B., Testa, C., Zorzan, A., Sabattoli, F., Beltramello, A., Soininen, H., & Laakso, M. P. (2002). Detection of grey matter loss in mild Alzheimer’s disease with voxel based morphometry. *Journal of Neurology Neurosurgery and Psychiatry*, 73(6), 657–664. <http://doi.org/10.1136/jnnp.73.6.657>
- Friston, K. J., Holmes, a, Poline, J. B., Price, C. J., & Frith, C. D. (1996). Detecting activations in PET and fMRI: levels of inference and power. *NeuroImage*, 4(3 Pt 1), 223–35. <http://doi.org/10.1006/nimg.1996.0074>
- Friston, K. J., Holmes, A. P., Worsley, K. J., Poline, J.-B., Frith, C. D., & Frackowiak, R. S. (1995). Statistical parametric maps in functional imaging: a general linear model approach. *Human Brain Mapping*, 2, 189–210. <http://doi.org/10.1002/hbm.460020402>
- Friston, K. J., Worsley, K. J., Frackowiak, R. S. J., Mazziotta, J. C., & Evans, A. C. (1994). Assessing the significance of focal activations using their spatial extent. *Human Brain Mapping*, 1(3), 210–220. <http://doi.org/10.1002/hbm.460010306>
- Gallea, C., Popa, T., García-Lorenzo, D., Valabregue, R., Legrand, A. P., Marais, L., ... Meunier, S. (2015). Intrinsic signature of essential tremor in the cerebello-frontal network. *Brain*, 138(10), 2920–2933. <http://doi.org/10.1093/brain/awv171>
- Glickman, M. E., Rao, S. R., & Schultz, M. R. (2014). False discovery rate control is a recommended alternative to Bonferroni-type adjustments in health studies. *Journal of Clinical Epidemiology*, 67(8), 850–857. <http://doi.org/10.1016/j.jclinepi.2014.03.012>
- Grimaldi, G., & Manto, M. (2013). Is essential tremor a purkinjopathy? The role of the cerebellar cortex in its pathogenesis. *Movement Disorders*, 28(13), 1759–1761. <http://doi.org/10.1002/mds.25645>

- Harasymiw, J. W., & Bean, P. (2001). Identification of heavy drinkers by using the early Detection of Alcohol Consumption Score. *Alcoholism: Clinical & Experimental Research*, 25(2), 228–236.
- He, N., Ling, H., Ding, B., Huang, J., Zhang, Y., Zhang, Z., ... Yan, F. (2015). Region-specific disturbed iron distribution in early idiopathic Parkinson's disease measured by quantitative susceptibility mapping. *Human Brain Mapping*, 36(11), 4407–4420. <http://doi.org/10.1002/hbm.22928>
- Heckova, E., Považan, M., Strasser, B., Hnilicová, P., Hangel, G. J., Moser, P. A., & Andronesi, O. C. (2017). Real-time Correction of Motion and Imager Instability Artifacts, *000*(0), 1–10.
- Helmich, R. C., Toni, I., Deuschl, G., & Bloem, B. R. (2013). The pathophysiology of essential tremor and parkinson's tremor. *Current Neurology and Neuroscience Reports*, 13(9). <http://doi.org/10.1007/s11910-013-0378-8>
- Hernandez-Castillo, C. R., Galvez, V., Diaz, R., & Fernandez-Ruiz, J. (2016). Specific cerebellar and cortical degeneration correlates with ataxia severity in spinocerebellar ataxia type 7. *Brain Imaging and Behavior*, 10(1), 252–257. <http://doi.org/10.1007/s11682-015-9389-1>
- Homayoon, N., Pirpamer, L., Frantl, S., Katschnig- Winter, P., Kögl, M., Seiler, S., ... Schwingenschuh, P. (2018). Nigral iron deposition in common tremor disorders. *Movement Disorders*, 34(1), 129–132. <http://doi.org/10.1002/mds.27549>
- Jain, S., Lo, S. E., & Louis, E. D. (2006). Common Misdiagnosis of a Common Neurological Disorder. *Archives of Neurology*, 63(8), 1100. <http://doi.org/10.1001/archneur.63.8.1100>
- Jakab, A., Molnár, P. P., Bogner, P., Béres, M., & Berényi, E. L. (2012). Connectivity-based parcellation reveals interhemispheric differences in the insula. *Brain Topography*, 25(3), 264–271. <http://doi.org/10.1007/s10548-011-0205-y>
- Kaiser, L. G., Young, K., Meyerhoff, D. J., Mueller, S. G., & Matson, G. B. (2008). A detailed analysis of localized J-difference GABA editing: theoretical and experimental study at 4 T. *NMR in Biomedicine*, 21(1), 22–32. <http://doi.org/10.1002/nbm.1150>
- Klaming, R., & Annese, J. (2014). Functional anatomy of essential tremor: Lessons from neuroimaging. *American Journal of Neuroradiology*, 35(8), 1450–1457. <http://doi.org/10.3174/ajnr.A3586>
- Krumpolec, P., Vallova, S., Slobodova, L., Tirpakova, V., Vajda, M., Schon, M., ... Ukropec, J. (2017). Aerobic-strength exercise improves metabolism and clinical state in Parkinson's disease patients. *Frontiers in Neurology*, 8(DEC), 1–12. <http://doi.org/10.3389/fneur.2017.00698>
- Langkammer, C., Pirpamer, L., Seiler, S., Deistung, A., Schweser, F., Frantl, S., ... Schwingenschuh, P. (2016). Quantitative Susceptibility Mapping in Parkinson's Disease. *PloS One*, 11(9), e0162460. <http://doi.org/10.1371/journal.pone.0162460>

- Lenka, A., Bhalsing, K. S., Panda, R., Jhunjhunwala, K., Naduthota, R. M., Saini, J., ... Pal, P. K. (2017). Role of altered cerebello-thalamo-cortical network in the neurobiology of essential tremor. *Neuroradiology*, *59*(2), 157–168. <http://doi.org/10.1007/s00234-016-1771-1>
- Lin, C.-H., Chen, C.-M., Lu, M.-K., Tsai, C.-H., Chiou, J.-C., Liao, J.-R., & Duann, J.-R. (2013). VBM Reveals Brain Volume Differences between Parkinson's Disease and Essential Tremor Patients. *Frontiers in Human Neuroscience*, *7*(June), 247. <http://doi.org/10.3389/fnhum.2013.00247>
- Louis, E. D. (2010). Essential tremor: evolving clinicopathological concepts in an era of intensive post-mortem enquiry. *The Lancet Neurology*, *9*(6), 613–622. [http://doi.org/10.1016/S1474-4422\(10\)70090-9](http://doi.org/10.1016/S1474-4422(10)70090-9)
- Louis, E. D. (2014). “Essential tremor” or “the essential tremors”: Is this one disease or a family of diseases? *Neuroepidemiology*, *42*(2), 81–89. <http://doi.org/10.1159/000356351>
- Louis, E. D. (2015). Utility of the hand-drawn spiral as a tool in clinical-epidemiological research on essential tremor: Data from four essential tremor cohorts. *Neuroepidemiology*, *44*(1), 45–50. <http://doi.org/10.1159/000371850>
- Louis, E. D. (2016). Non-motor symptoms in essential tremor: A review of the current data and state of the field. *Parkinsonism and Related Disorders*, *22*(2016), S115–S118. <http://doi.org/10.1016/j.parkreldis.2015.08.034>
- Louis, E. D., Faust, P. L., Vonsattel, J. P. G., Honig, L. S., Rajput, A., Robinson, C. A., ... Hernandez, N. (2007). Neuropathological changes in essential tremor: 33 Cases compared with 21 controls. *Brain*, *130*(12), 3297–3307. <http://doi.org/10.1093/brain/awm266>
- Louis, E. D., Ford, B., Lee, H., Andrews, H., & Cameron, G. (1998). Diagnostic Criteria for Essential Tremor. *Archives of Neurology*, *55*(6), 823–828. <http://doi.org/10.1001/archneur.55.6.823>
- Louis, E. D., Hernandez, N., Dyke, J. P., Ma, R., & Dydak, U. (2016). Effect of Primidone on Dentate Nucleus Gamma-aminobutyric Acid Concentration in Patients with Essential Tremor. *Clin Neuropharmacol.*, *39*(1), 24–28. <http://doi.org/10.1097/WNF.000000000000127>
- Louis, E. D., Hernandez, N., Dyke, J. P., Ma, R. E., & Dydak, U. (2018). In Vivo Dentate Nucleus Gamma-aminobutyric Acid Concentration in Essential Tremor vs. Controls. *Cerebellum*, *17*(2), 165–172. <http://doi.org/10.1007/s12311-017-0891-4>
- Louis, E. D., Huang, C. C., Dyke, J. P., Long, Z., & Dydak, U. (2014). Neuroimaging studies of essential tremor: how well do these studies support/refute the neurodegenerative hypothesis? *Tremor and Other Hyperkinetic Movements (New York, N.Y.)*, *4*, 235. <http://doi.org/10.7916/D8DF6PB8>

- Louis, E. D., Lee, M., Babij, R., Ma, K., Cortés, E., Vonsattel, J. P. G., & Faust, P. L. (2014). Reduced Purkinje cell dendritic arborization and loss of dendritic spines in essential tremor. *Brain*, *137*(12), 3142–3148. <http://doi.org/10.1093/brain/awu314>
- Louis, E. D., & Ottman, R. (2014). How many people in the USA have essential tremor? Deriving a population estimate based on epidemiological data. *Tremor and Other Hyperkinetic Movements (New York, N.Y.)*, *4*, 259. <http://doi.org/10.7916/D8TT4P4B>
- Louis, E. D., Shungu, D. C., Chan, S., Mao, X., Jurewicz, E. C., & Watner, D. (2002). Metabolic abnormality in the cerebellum in patients with essential tremor: A proton magnetic resonance spectroscopic imaging study. *Neuroscience Letters*, *333*(1), 17–20. [http://doi.org/10.1016/S0304-3940\(02\)00966-7](http://doi.org/10.1016/S0304-3940(02)00966-7)
- Mayka, M. A., Corcos, D. M., Leurgans, S. E., & Vaillancourt, D. E. (2006). Three-dimensional locations and boundaries of motor and premotor cortices as defined by functional brain imaging: A meta-analysis. *NeuroImage*, *31*(4), 1453–1474. <http://doi.org/10.1016/j.neuroimage.2006.02.004>
- Merker, B., & Podell, K. (2011). Grooved Pegboard Test. In J. S. Kreutzer, J. DeLuca, & B. Caplan (Eds.), *Encyclopedia of Clinical Neuropsychology* (pp. 1176–1178). New York, NY: Springer New York. [http://doi.org/10.1007/978-0-387-79948-3\\_187](http://doi.org/10.1007/978-0-387-79948-3_187)
- Mescher, M., Merkle, H., Kirsch, J., Garwood, M., & Gruetter, R. (1998). Simultaneous in vivo spectral editing and water suppression. *NMR in Biomedicine*, *11*(6), 266–272. [http://doi.org/10.1002/\(SICI\)1099-1492\(199810\)11:6<266::AID-NBM530>3.0.CO;2-J](http://doi.org/10.1002/(SICI)1099-1492(199810)11:6<266::AID-NBM530>3.0.CO;2-J)
- Mullins, P. G., McGonigle, D. J., O’Gorman, R. L., Puts, N. A. J., Vidyasagar, R., Evans, C. J., ... Wilson, M. (2014). Current practice in the use of MEGA-PRESS spectroscopy for the detection of GABA. *NeuroImage*, *86*, 43–52. <http://doi.org/10.1016/j.neuroimage.2012.12.004>
- Muthuraman, M., Raethjen, J., Koirala, N., Anwar, A. R., Mideksa, K. G., Elble, R., ... Deuschl, G. (2018). Cerebello-cortical network fingerprints differ between essential, Parkinson’s and mimicked tremors. *Brain*, *141*(6), 1770–1781. <http://doi.org/10.1093/brain/awy098>
- Nasreddine, Z., Phillips, N., Bédirian, V., Charbonneau, S., Whitehead, V., Collin, I., ... Chertkow, H. (2005). The Montreal Cognitive Assessment, MoCA: a brief screening tool for mild cognitive impairment. *Journal of the American Geriatrics Society*, *53*(4), 695–699. <http://doi.org/10.1111/j.1532-5415.2005.53221.x>
- Nicoletti, V., Cecchi, P., Frosini, D., Pesaresi, I., Fabbri, S., Diciotti, S., ... Ceravolo, R. (2015). Morphometric and functional MRI changes in essential tremor with and without resting tremor. *Journal of Neurology*, *262*(3), 719–728. <http://doi.org/10.1007/s00415-014-7626-y>
- Novellino, F., Cherubini, A., Chiriaco, C., Morelli, M., Salsone, M., Arabia, G., & Quattrone, A. (2013). Brain iron deposition in essential tremor: A quantitative 3-tesla magnetic resonance imaging study. *Movement Disorders*, *28*(2), 196–200. <http://doi.org/10.1002/mds.25263>

- O’Gorman Tuura, R. L., Baumann, C. R., & Baumann-Vogel, H. (2018). Beyond dopamine: GABA, glutamate, and the axial symptoms of Parkinson disease. *Frontiers in Neurology*, 9(SEP), 1–9. <http://doi.org/10.3389/fneur.2018.00806>
- Oz, G. (2016). *Magnetic Resonance Spectroscopy of Degenerative Brain Diseases*. <http://doi.org/10.1007/978-3-319-33555-1>
- Pesch, B., Casjens, S., Woitalla, D., Dharmadhikari, S., Edmondson, D., Zella, M., ... Dydak, U. (2019). Impairment of Motor Function Correlates with Neurometabolite and Brain Iron Alterations in Parkinson’s Disease. *Cells*, 8(2), 96. <http://doi.org/10.3390/cells8020096>
- Provencher, S. W. (1993). Estimation of metabolite concentrations from localized in vivo proton NMR spectra. *Magnetic Resonance in Medicine*, 30(6), 672–679. <http://doi.org/10.1002/mrm.1910300604>
- Puts, N. A. J., Barker, P. B., & Edden, R. A. E. (2013). Measuring the longitudinal relaxation time of GABA in vivo at 3 Tesla. *Journal of Magnetic Resonance Imaging*, 37(4), 999–1003. <http://doi.org/10.1002/jmri.23817>
- Quattrone, A., Cerasa, a., Messina, D., Nicoletti, G., Hagberg, G. E., Lemieux, L., ... Salsone, M. (2008). Essential head tremor is associated with cerebellar vermis atrophy: A volumetric and voxel-based morphometry MR imaging study. *American Journal of Neuroradiology*, 29(9), 1692–1697. <http://doi.org/10.3174/ajnr.A1190>
- R Core Team. (2017). R: A Language and Environment for Statistical Computing. Vienna, Austria. Retrieved from <https://www.r-project.org/>
- Rajput, A. H., Robinson, C. A., Rajput, M. L., Robinson, S. L., & Rajput, A. (2012). Essential tremor is not dependent upon cerebellar Purkinje cell loss. *Parkinsonism and Related Disorders*, 18(5), 626–628. <http://doi.org/10.1016/j.parkreldis.2012.01.013>
- Schmahmann, J. D., Doyon, J., McDonald, D., Holmes, C., Lavoie, K., Hurwitz, A. S., ... Petrides, M. (1999). Three-dimensional MRI atlas of the human cerebellum in proportional stereotaxic space. *Neuroimage*, 10(3), 233–260. Retrieved from <http://0-apps.isiknowledge.com.mercury.concordia.ca/WoS/CIW.cgi>
- Sharifi, S., Nederveen, A. J., Booij, J., & van Rootselaar, A.-F. (2014). Neuroimaging essentials in essential tremor: a systematic review. *NeuroImage. Clinical*, 5, 217–31. <http://doi.org/10.1016/j.nicl.2014.05.003>
- Shin, H., Lee, D. K., Lee, J. M., Huh, Y. E., Youn, J., Louis, E. D., & Cho, J. W. (2016). Atrophy of the Cerebellar Vermis in Essential Tremor: Segmental Volumetric MRI Analysis. *Cerebellum*, 15(2), 174–181. <http://doi.org/10.1007/s12311-015-0682-8>
- Statton, M. A., Vazquez, A., Morton, S. M., Vasudevan, E. V. L., & Bastian, A. J. (2018). Making Sense of Cerebellar Contributions to Perceptual and Motor Adaptation. *Cerebellum*, 17(2), 111–121. <http://doi.org/10.1007/s12311-017-0879-0>

- Symanski, C., Shill, H. A., Dugger, B., Hentz, J. G., Adler, C. H., Jacobson, S. A., ... Beach, T. G. (2014). Essential tremor is not associated with cerebellar Purkinje cell loss. *Movement Disorders*, 29(4), 496–500. <http://doi.org/10.1002/mds.25845>
- Tarakad, A., & Jankovic, J. (2018). Reviews Essential Tremor and Parkinson ' s Disease : Exploring the Relationship, 1–10. <http://doi.org/10.7916/D8MD0GVR>
- Träber, F., Block, W., Lamerichs, R., Gieseke, J., & Schild, H. H. (2004). 1H Metabolite Relaxation Times at 3.0 Tesla: Measurements of T1 and T2 Values in Normal Brain and Determination of Regional Differences in Transverse Relaxation. *Journal of Magnetic Resonance Imaging*, 19(5), 537–545. <http://doi.org/10.1002/jmri.20053>
- Tremor Fact Sheet. (2017). Retrieved from <https://www.ninds.nih.gov/Disorders/Patient-Caregiver-Education/Fact-Sheets/Tremor-Fact-Sheet>
- Ulla, M., Bonny, J. M., Ouchchane, L., Rieu, I., Claise, B., & Durif, F. (2013). Is R2\* a New MRI Biomarker for the Progression of Parkinson's Disease? A Longitudinal Follow-Up. *PLoS ONE*, 8(3), 1–8. <http://doi.org/10.1371/journal.pone.0057904>
- Ward, R. J., Zucca, F. A., Duyn, J. H., Crichton, R. R., & Zecca, L. (2014). The role of iron in brain ageing and neurodegenerative disorders. *The Lancet Neurology*, 13(10), 1045–1060. [http://doi.org/10.1016/S1474-4422\(14\)70117-6](http://doi.org/10.1016/S1474-4422(14)70117-6)
- Zecca, L., Youdim, M. B. H., Riederer, P., Connor, J. R., & Crichton, R. R. (2004). Iron, brain ageing and neurodegenerative disorders. *Nature Reviews Neuroscience*, 5(11), 863–873. <http://doi.org/10.1038/nrn1537>